https://doi.org/10.5194/bg-2021-164
Preprint. Discussion started: 28 June 2021

Biogeosciences Discussions

Nutrient transport and transformation in macrotidal estuaries of the French Atlantic coast: a modelling approach using C-GEM

Xi Wei[1*], Josette Garnier[1*], Vincent Thieu[1], Paul Passy[2], Romain Le Gendre[3], Gilles Billen[1], Maia Akopian[4], and Goulven Gildas Laruelle[5]

1 UMR Metis 7619, Sorbonne Université, CNRS EPHE, 4 Place Jussieu, Paris, 75005, France
2 UMR 8586 PRODIG, Université de Paris, 8 rue Albert Einstein, 75013 Paris, France
3 Ecosystèmes et Aquaculture Durable, Unité de Recherche Lagons, IFREMER, Noumea, 98897, New-Caledonia
4 Department of Research and Scientific Support, French Biodiversity Agency (OFB), 5 square Félix Nadar, 94300 Vincennes, France
5 Department of Geosciences, Environment and Society, Université Libre de Bruxelles, Brussels, 1050, Belgium

Correspondence to: Xi Wei (xi.wei@upmc.fr; xi.wei_fr@hotmail.com); Josette Garnier (josette.garnier@upmc.fr).

Abstract: Estuaries are key reactive ecosystems along the land–ocean aquatic continuum, with significant ecological and economic value. However, they have been facing strong morphological management changes as well as increased nutrient and contaminant inputs, possibly leading to ecological problems such as coastal eutrophication. Therefore, it is necessary to quantify the ingoing and outgoing fluxes of the estuaries, their retention capacity, and estuarine eutrophication potential. A 1-D Carbon–Generic Estuary Model (C-GEM) was used to simulate the transient hydrodynamics, transport, and biogeochemistry for estuaries with different sizes and morphologies along the French Atlantic coast during the period 2014–2016 using readily available geometric, hydraulic, and biogeochemical data. These simulations allowed us to evaluate the budgets of the main nutrients (phosphorus [P], nitrogen [N], silica [Si]) and total organic carbon (TOC), and their imbalance with respect to estuarine eutrophication potential. Cumulated average annual fluxes to the Atlantic coast from the seven estuaries studied were 9.6 kt P yr^{-1}, 259 kt N yr^{-1}, 304 kt Si yr^{-1}, and 145 kt C yr^{-1}. Retention rates varied depending on the estuarine residence times, ranging from 0–27%, 0–34%, 2–39%, and 8–96% for TP, TN, DSi, and TOC, respectively. Large-scale estuaries had higher retention rates than medium and small estuaries, which we interpreted in terms of estuarine residence times. As shown by the indicator of eutrophication potential (ICEP), there might be a risk of coastal eutrophication, i.e., the development of nonsiliceous algae that is potentially harmful to the systems studied due to the excess TN over DSi.

Key words: estuary; biogeochemical process; retention; modelling; French Atlantic coast.

1. Introduction

Nutrient transport and transformation along the land–ocean aquatic continuum are receiving increasing attention due to their role in the global nutrient cycle and budget (Howarth et al., 2011, 1991). The estuary is a partly enclosed body of water, characterized by mixing of salty ocean water with fresh river water (Pritchard, 1967; Vilas et al., 2021), and is an important reactive ecosystem along the land–ocean continuum (Crossland et al., 2005; Regnier et al., 2013). Morphologically, an

https://doi.org/10.5194/bg-2021-164
Preprint. Discussion started: 28 June 2021

estuary is an important component connecting land to ocean (Dürr et al., 2011). Freshwater, suspended particulate matter (SPM), nutrients, and contaminations from watersheds are transferred to the sea and transformed through these interface ecosystems. Ecologically, estuaries are among the most productive ecosystems in the world due to dynamic biogeochemical processes and they ensure many ecological functions that need to be preserved (Barbier et al., 2011; Liquete et al., 2013; Pozdnyakov et al., 2017). They contribute to vegetation growth (aquatic angiosperms, salt marshes, mangroves, etc.) and animal production (e.g., invertebrates, fish breeding and nursing, bird reproduction and feeding as well as resting areas). Economically, aquaculture develops around the estuary; agriculture, tourism (port cities), industry and import/export logistics are also active within estuarine basins. Estuarine and coastal ecosystems throughout the world are some of the most heavily used and threatened natural systems (Barbier et al., 2011), and they are facing increasing anthropogenic impacts given that they are the receptacle of all the contaminants and nutrients from the upper river watershed (Garnier et al., 2021), from both point sources (urban and industrial wastewater) and diffuse sources (agriculture). Additionally, harbors, channelization, and flood protection structures have changed not only the geomorphology of the estuaries, but also their hydrological and biogeochemical behaviors (Romero et al., 2016). These impacts may well be at the heart of critical environmental issues such as estuary and coastal eutrophication. Eutrophication is the perturbation of an aquatic ecosystem by excessive nutrient enrichment and its manifestations may take various forms, including harmful algal blooms (Glibert, 2020), which can cause damage to coastal fisheries (Husson et al., 2016). Moreover, overproduction of these harmful algal blooms, which are not suitable for consumption by zooplankton and benthic invertebrates, possibly leads to hypoxia of the bottom water layers (Garnier et al., 2021). Due to the importance of these different aspects of estuaries, their environmental situations and problems are receiving increasing attention from both researchers and stakeholders.

In order to estimate and potentially control the potential eutrophication or/and hypoxia, the biogeochemical processes (nutrient transport and transformation) in the estuarine systems should be understood. Therefore, accurate quantification of estuarine nutrient fluxes (inputs and outputs) is necessary for evaluating the “retention” of the system, i.e., the amount of nutrient either sequestered within the estuary and its sediment or eliminated from the system to the atmosphere. In another words, estuarine retention rates reflect the internal biogeochemical processes and reactions along the estuary, such as uptake, losses, transformation, changes in storage, mineralization, and degradation. Nutrient retention rates can be mainly influenced by estuarine geomorphology, the surrounding wetlands (most particularly intertidal areas), river discharge, the turbidity maximum zone, estuarine residence time, and other physical forcings (Arndt et al., 2009; Perez et al., 2011). Thus, gaining insight into the retention capacities of estuaries can help understand the biogeochemical intensity within the estuary and also manage the nutrient imports from the upstream river basins and hence nutrient exports to the seas.

Although the estuarine surface areas are much smaller than those of river networks and coastal marine systems, studying the estuarine ecological function is also complex due to the influences from both the riverine and marine aspects, such as the tide, salinity gradient, estuarine turbidity maximum zone, and hydromorphology (Regnier et al., 1998). To study the estuarine biogeochemical processes, common approaches include in-situ sampling (Coynel et al., 2016; Kaiser et al., 2013; Michel et al., 2000; Modéran et al., 2012; Nguyen et al., 2019; Perez et al., 2011; Savoye et al., 2012) and/or numerical modelling

https://doi.org/10.5194/bg-2021-164
Preprint. Discussion started: 28 June 2021

(Arndt et al., 2009; Garnier et al., 2007; Hu and Li, 2009; Laruelle et al., 2019; Ménesguen et al., 2019; Nguyen et al., 2021; Romero et al., 2019). However, direct observations do not allow to quantify nutrient fluxes in macrotidal estuaries because the oscillatory tidal flux is several orders of magnitude larger than the ecologically and biogeochemically-relevant retention flux (Regnier et al., 1998), despite mixing curves have been useful for interpreting in situ observations and nutrient dynamics. Moreover, the retention flux generally falls within the range of measurement uncertainties (Arndt et al., 2009; Jay et al., 1997; Regnier et al., 1998). Numerical models combined with limited observed data can fill the gap in understanding nutrient dynamics and offer insight into past and future scenarios in response to environmental and human changes (such as land use changes and agricultural practices), and climate change (Billen and Garnier, 1997; Garnier et al., 2021; Ménesguen et al., 2018b). In addition, simulations can be carried out at large spatial and temporal scales. In particular, they can realistically represent the spatial variability within estuaries and provide a global view of the whole basin (land–ocean continuum) by chaining estuarine with river basin models (Laruelle et al., 2019) as well as with coastal zone models (Garnier et al., 2019; Ménesguen et al., 2018b; Romero et al., 2019).

In recent decades, many estuarine numerical models have been applied to disentangle the complex physical and biogeochemical processes, such as 3-D models (Lajaunie-Salla et al., 2017; Romero et al., 2019; Wild-Allen et al., 2013), 2-D models (Arndt et al., 2011; Vanderborght et al., 2007), 1-D models (Hofmann et al., 2008; Volta et al., 2014), and box models (Garnier et al., 2008, 2010b; Verri et al., 2021). However, 3-D models require massive data for calibration and high computing performance to resolve the complex processes occurring in estuaries on relevant spatial and temporal scales. On the opposite side of the complexity spectrum, box models might neglect the transient behavior of the flow and scalar fields and by nature cannot reproduce the complex hydrology of estuarine environments, consequently causing large errors in flux estimations (Arndt et al., 2009). The Carbon-Generic Estuary Model (C-GEM; Volta et al., 2014) used in this study is a depth-averaged 1-D model that has been developed to handle the main obstacles to the application of estuarine models on a regional or global scale (Laruelle et al., 2017). The generic implementation of the C-GEM model relies on a limited amount of basic information to describe estuarine geometry, hydrodynamic information, and the inputs to estuaries, and then produces annual to multi-decadal simulations. C-GEM has already been applied to one tropical estuary (Nguyen et al., 2021) and several temperate estuaries and has provided satisfactory simulations of nutrient transport and biogeochemical processes despite the simplification of the estuarine geometry (Laruelle et al., 2017, 2019; Volta et al., 2014, 2016a). An extensive description of C-GEM is presented in Volta et al. (2014, 2016a).

The French estuaries along the northeastern Atlantic coast studied herein have been subjected to nutrient enrichment for many years (Garnier et al., 2019; Ménesguen et al., 2019; Ratmaya et al., 2019). Therefore, the objectives of this paper are to: (i) evaluate the nutrient delivery of estuaries from the French Atlantic coast to the sea using the C-GEM modeling approach; (ii) quantify the retention rates of these estuaries; and (iii) analyze the coastal eutrophication potential. The first part of the paper presents longitudinal results averaged over a tidal cycle, including salinity and SPM, nutrients and phytoplankton biomass, under different hydrological years (2014–2016) for seven selected estuaries of different sizes and anthropization degrees/levels. Then the annual input–output budgets of nutrients is provided in order to quantify the retention rates of these

https://doi.org/10.5194/bg-2021-164
Preprint. Discussion started: 28 June 2021

estuaries according to their specific characteristics (size, degree of hydromorphological management, anthropogenic pressures, etc.).

2. Materials and Methods

2.1. Study Area

This study focused on seven estuaries (from north to south: Somme, Seine, Vilaine, Loire, Charente, Gironde, and Adour) along the French Atlantic coast (Figure 1). These estuaries embody a wide range of morphological and hydrological settings representative of the region in terms of length, width, residence time, convergence length, tidal amplitude, and length of saline intrusion. Considering these features, they were divided into three large estuaries (the Seine, Loire, and Gironde), two medium-size estuaries (Charente and Adour), and two small ones (Somme and Vilaine). Their geometric properties are presented in Table 1. They are characterized as semi-diurnal and macrotidal estuaries, with an average tidal range from 3.3 m to 5.1 m (Table 1).

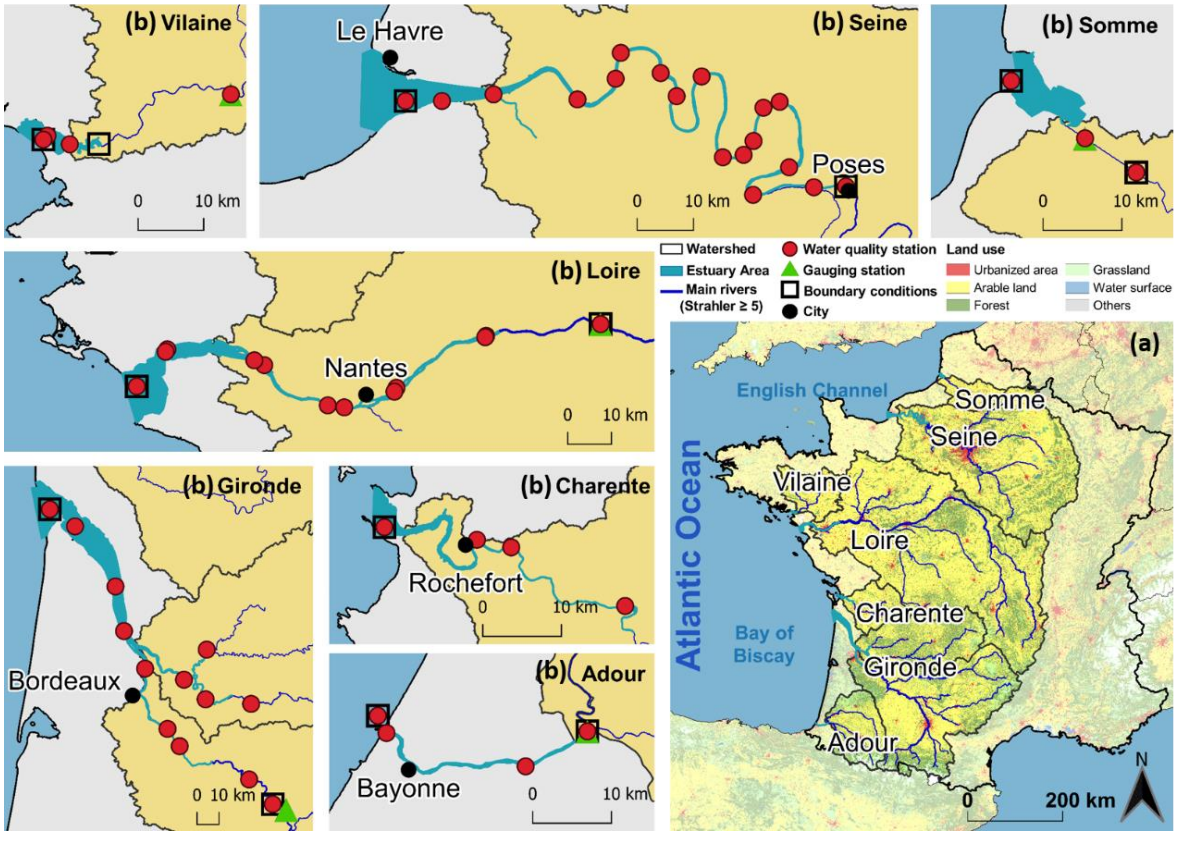

Figure 1 (a) Map of estuaries studied along the French Atlantic coast. (b) Panels for each estuary indicate the locations of the gauging stations and the water quality stations used in this study.

https://doi.org/10.5194/bg-2021-164
Preprint. Discussion started: 28 June 2021

Table 1 Geometric properties of the estuaries studied.

Estuary	Seine	Loire	Gironde	Charente	Adour	Somme	Vilaine
Estuary length (km)	166	122	202	50	34	18	10
River basin area (km^2)	65,000	111,436	51,343	7598	14,832	5560	10,498
Estuary basin area (km^2)	11,843	6891	31,459	2327	2122	820	237
Depth at estuary mouth (m)	4.7	10.0	12.0	8.0	10.0	9.0	5.0
Mean tidal range (m)	5.1	4.0	3.7	4.3	3.3	3.9	3.9
Width at estuary mouth (km)	10.0	10.7	12.0	1.8	0.4	3.5	2.3
Width at inflection point 1 (km)	0.48	1.5	3.6	0.3	-	0.35	-
Width at inflection point 2 (km)	-	0.35	-	-	-	-	-
Convergence length (km)	10.7	12.0	48.0	3.5	40.0	3.2	15.0
Convergence length in the middle of the estuary (km)	-	21.0	-	-	-	-	-
Convergence length in the upper estuary (km)	105.5	600.0	19.0	21.0	-	4.0	-

Note: The geometry information (length, surface area, and width) was derived from remote sensing images through the Esri Ocean layer in Geographic Information System (GIS). Depths were obtained from (Defontaine et al., 2019; Goubert et al., 2019; Laruelle et al., 2019; McLean et al., 2019; Normandin et al., 2019; Toublanc et al., 2015).

These estuaries receive nutrient deliveries from the upper river basins with different land uses and population densities (Table 2): for example, the Seine, Vilaine, Loire, and Charente river basins are dominated by agricultural activities, sustaining a large proportion of the national livestock and/or production of crop agriculture (Billen and Garnier, 2007; Ménesguen et al., 2018a; Ratmaya et al., 2019). The percentages of different land use types for each basin are presented in Table 2. The intensive agriculture and urbanization within the estuarine basins studied induced eutrophication, especially those of the north half of the French Atlantic coast, regarded as nutrient-enriched (Garnier et al., 2019; Ménesguen et al., 2019; Ratmaya et al., 2019).

Table 2 Population density (INSEE, 2014) and land use type percentage (UE-SOeS CORINE Land Cover, 2018) of the river basin of the systems studied.

Basin	Area km^2	Population density inhab km^{-2}	Arable land %	Urban %	Grassland %	Forest %	Water surface %	Others %
Seine	65,000	256.9	66%	8%	1%	25%	1%	0%
Loire	111,436	74.6	72%	4%	1%	21%	1%	0%
Gironde	51,343	95.6	56%	3%	6%	33%	1%	1%
Charente	7598	79.0	77%	5%	1%	18%	0%	0%
Adour	14,832	72.8	48%	4%	16%	27%	0%	4%
Somme	5560	115.1	84%	7%	0%	8%	1%	1%
Vilaine	10,498	106.7	82%	6%	1%	11%	0%	0%

2.2. Data Collection

The measured data used in this study to calibrate and validate the model, as well as to determine the upstream limit conditions, include discharge (Q), salinity (Sal), suspended particulate matter (SPM), and water quality variables, i.e., phosphate (PO_4), ammonium (NH_4), nitrate (NO_3), dissolved silica (DSi), dissolved oxygen (DO), total (particulate and

https://doi.org/10.5194/bg-2021-164
Preprint. Discussion started: 28 June 2021

dissolved) organic carbon (TOC), and chlorophyll a (Chl-a), as an indicator of phytoplankton biomass.

Daily discharge data were obtained from the national Banque Hydro database (http://www.hydro.eaufrance.fr/). Water quality variables were collected from the national database: (1) the French Water Agencies through the NAIADES portal (http://naiades.eaufrance.fr/) for the physicochemical parameters of surface waters; (2) the REPHY (REPHY, 2021) database (https://www.seanoe.org/data/00361/47248/) specifically for the monitoring of phytoplankton for the estuarine and marine parts; and (3) the SOMLIT database (https://www.somlit.fr/) for coastal and estuarine water quality parameters. The temporal resolution of the water quality data acquired is generally monthly or bimonthly. Chl-a concentrations were usually available only from March to September (main phytoplankton growth period). The gauging stations and water quality stations are located in Figure 1(b).

The data for the marine boundaries were extracted from outputs of simulations performed by a coastal marine model ECO-MARS3D (Cugier et al., 2005b; Lazure and Dumas, 2008; Ménesguen et al., 2019), providing water elevation, temperature, salinity, SPM, PO_4, NH_4, NO_3, DSi, DO, TOC, and phytoplankton (Phy) at 4-km spatial and hourly temporal resolutions.

The use of the above database is detailed in section 2.3.3.

2.3. Modelling Approach and Setting

2.3.1. C-GEM

In this study, the C-GEM (Carbon Generic Estuarine Model) was used for modeling nutrient transport and transformation for the selected estuaries. The C-GEM is a depth-averaged 1-D process-based model designed to simulate estuarine hydrodynamics, transport, and the biogeochemistry of alluvial estuaries with relatively little data and computation demand (Volta et al., 2014, 2016b). It has already been applied to a number of estuaries along the North Sea and the English Channel in Western Europe (Laruelle et al., 2019; Volta et al., 2016b), along the North Atlantic Ocean in North America (Laruelle et al., 2017), and to the Saigon River estuary in Southeast Asia (Nguyen et al., 2021). These various applications provided good evidence of the ability of the model to capture and reproduce carbon and nutrient transport and transformation as well as carbon dioxide (CO_2) exchange with the atmosphere.

2.3.2. Numerical Schemes

C-GEM is based on the premise that geometry and hydrodynamics exert first-order control on the estuarine transport and biogeochemical processes (Volta et al., 2014). It uses idealized geometry (defined by the estuarine width at the mouth, convergence length, channel depth profile; see Volta et al., 2014 for details) and hydrodynamics (such as river discharge and tidal amplitude) that can be gained from remote sensing images using Geographic Information Software (GIS) and readily available data sets (Table 1).

The biogeochemical reaction network includes SPM settling and erosion, the air–water gas exchange for oxygen (O_2) and carbon dioxide (CO_2), nitrification, denitrification, primary production, phytoplankton mortality, and aerobic degradation of

https://doi.org/10.5194/bg-2021-164
Preprint. Discussion started: 28 June 2021

organic matter (see Volta et al. (2014a, 2016a) for detailed descriptions and mathematical formulations). Essential state variables are used in the simulations, as are those gathered above (mentioned in section 2.2: DO, NH_4, NO_3, PO_4, DSi, TOC, and diatom (Dia) and non-diatom (nDia)) pools are therefore considered in this study and schematized in Figure 2. Note that, in this study, the inorganic carbon module of C-GEM (which includes the explicit calculation of dissolved inorganic carbon, alkalinity, pCO_2, and pH) described in Volta et al. (2014) was not activated. While C-GEM does not yet include an explicit benthic compartment, a net burial term was applied to the particulate state variables of the model, namely: Dia, nDia, and TOC. This term provides a first-order representation of the permanent removal of particulate material through sediment accumulation. It is applied to phytoplankton and TOC, proportionally to their concentration and inversely proportionally to the depth of the water column, using a constant settling rate of 1 m d^{-1} for phytoplankton and 0.4 m d^{-1} for TOC.

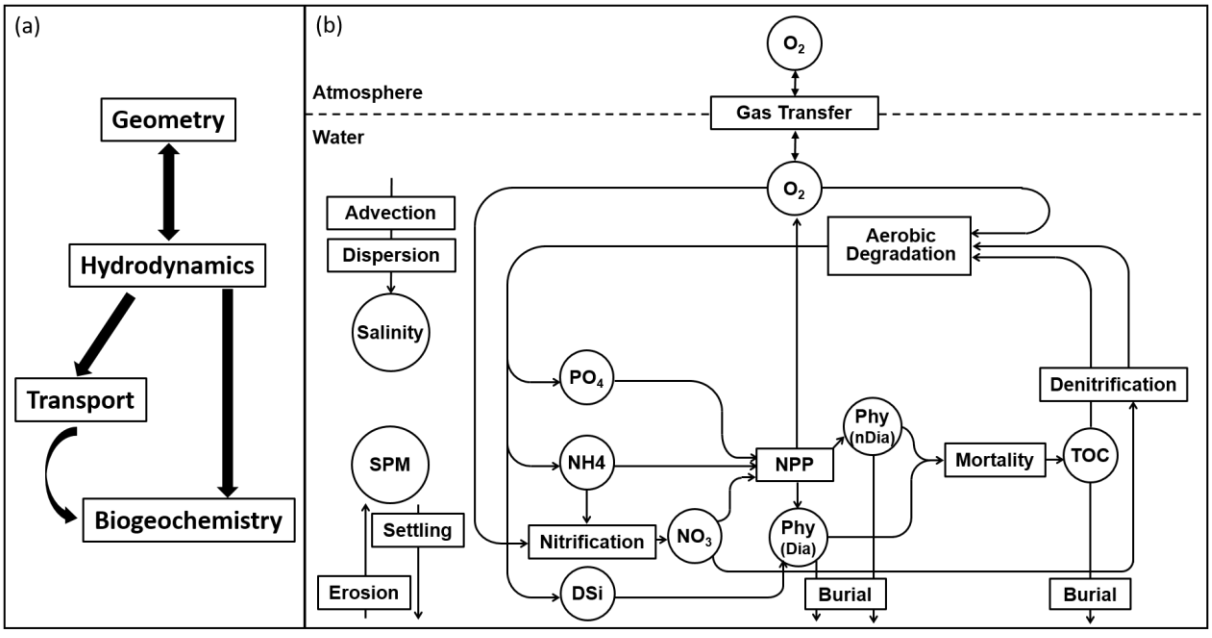

Figure 2 (a) The C-GEM concept. (b) Conceptual scheme of the biogeochemical module used in C-GEM in this study: a circle represents the state variables while a rectangle represents the processes; Dia corresponds to diatoms.

2.3.3. Forcings and Boundary Conditions

C-GEM is constrained by a set of riverine and marine boundary conditions. The riverine boundary conditions include river discharge (Q), SPM, and the state variables of water quality concentrations, which were linearly interpolated to obtain the daily values between the adjacent available measurements (Table 3). The marine boundary conditions include water elevation, water temperature, salinity, and the same water quality variables extracted from ECO-MARS3D at an hourly temporal resolution that allows capturing the tidal cycle. SPMs for the marine boundary conditions were collected from REPHY (REPHY, 2021) and linearly interpolated to obtain the data at the required time scale (Table 3). The annual means of boundary conditions are summarized in Table 4.

https://doi.org/10.5194/bg-2021-164
Preprint. Discussion started: 28 June 2021

Table 3 State variables in C-GEM and the boundary conditions.

State variable (abbreviation)	Unit in C-GEM	Marine boundary condition		Riverine boundary condition	
		Source	Timestep	Source	Timestep
Discharge (Q)	m^3/s	-	-	NAIADES	daily
Water elevation	m	ECO-MARS3D	hourly	-	-
Water temperature	℃	ECO-MARS3D	hourly	-	-
Salinity (Sal)	-	ECO-MARS3D	hourly	NAIADES	daily
Suspended particulate matter (SPM)	g L^{-1}	REPHY	hourly	NAIADES	daily
Phosphate (PO_4)	µmol P L^{-1}	ECO-MARS3D	hourly	NAIADES	daily
Ammonium (NH_4)	µmol N L^{-1}	ECO-MARS3D	hourly	NAIADES	daily
Nitrate (NO_3)	µmol N L^{-1}	ECO-MARS3D	hourly	NAIADES	daily
Dissolved silica (DSi)	µmol Si L^{-1}	ECO-MARS3D	hourly	NAIADES	daily
Total organic carbon (TOC)	µmol C L^{-1}	ECO-MARS3D	hourly	NAIADES	daily
Dissolved oxygen (DO)	µmol O_2 L^{-1}	ECO-MARS3D	hourly	NAIADES	daily
Phytoplankton (Phy)	µg L^{-1}	ECO-MARS3D	hourly	NAIADES	daily

In this study, the Dordogne River, a tributary of the Gironde estuary, which contributes ~40% discharge to the estuary, was considered as an upstream condition. The inputs from the Dordogne tributary include daily Q and the same water quality variables for riverine boundary conditions (Table 3). Intermittent observed water quality data were also interpolated to daily values.

2.3.4. Point Sources

The discharge from waste water treatment plants (WWTPs) was taken into account as point sources in the model. The WWTPs from the largest estuarine cities (above 50,000 inhabitants) were considered: Rouen, Nantes, Rochefort, Bordeaux, and Bayonne on the Seine, Loire, Charente, Gironde, and Adour rivers, respectively. Fluxes from WWTPs to estuaries were calculated based on the loads treated in each WWTP (expressed in inhabitant equivalents), the identification of treatment types and assuming specific per capita emissions (after appropriate treatment) of SPM, PO_4, NH_4, NO_3, DSi, TOC, DO (state variables of the model), with an average water release of 150 L $inhab^{-1}$ day^{-1} (Table 4).

Table 4 Annual mean of inputs (riverine boundary conditions) and point source (waste water treatment plants (WWTPs)) for the estuaries studied.

Estuary	Q m^3 s^{-1}	Sal psu	SPM mg L^{-1}	PO_4 mgP L^{-1}	NH_4 mgN L^{-1}	NO_3 mgN L^{-1}	DSi mgSi L^{-1}	TOC mgC L^{-1}	DO mgO_2 L^{-1}	Chl-a ug L^{-1}
Riverine boundary										
Seine	499.4±282.5	-	21.5±20.2	0.102±0.034	0.149±0.276	4.9±0.8	3.7±0.7	3.5±0.7	9.4±1.6	2.1±1.2
Loire	808.1±619.3	-	19.4±11.9	0.034±0.019	0.017±0.011	3.0±0.5	5.3±1.1	5.6±1.9	10.2±1.5	9.3±7.6
Gironde (without Dordogne)	521±386.7	-	19.6±26.5	0.034±0.013	0.052±0.036	1.6±0.6	2.9±0.9	2.5±0.7	9.8±1.5	1.8±3.1
*Dordogne**	*303.4±261.7*	-	*827.0±1460.4*	*0.043±0.020*	*0.047±0.092*	*1.5±0.3*	*4.4±0.8*	*3.2±1.0*	*9.2±2.2*	*2.8±3.2*
Charente	77.3±85.1	-	9.5±8.5	0.036±0.012	0.052±0.023	5.4±1.0	5.2±1.3	2.6±0.8	9.1±1.4	1.4±0.4
Adour	324.9±293.2	-	20.9±26.9	0.039±0.018	0.080±0.041	1.6±0.5	2.7±0.3	2.5±0.9	9.4±1.2	1.2±0.4
Somme	48.2±7.5	-	9.0±6.8	0.033±0.016	0.063±0.024	4.4±0.6	8.4±1.2	2.6±0.3	9.8±1.6	2.1±2.3
Vilaine	95.6±140.0	-	12.6±6.7	0.034±0.018	0.045±0.026	4.6±2.0	6.7±0.9	3.5±1.4	10.3±1.4	14.5±14.8
Marine boundary										
Seine	-	15.1±3.3	3.6±2.5	0.071±0.020	0.027±0.027	2.8±0.5	1.9±0.4	0.7±0.1	9.6±1.1	6.7±1.5
Loire	-	23.1±2.4	43.1±37.6	0.039±0.008	0.015±0.007	1.0±0.4	1.9±0.4	0.7±0.3	7.3±1.5	1.9±1.4
Gironde	-	30.1±2.1	36.5±20.2	0.021±0.006	0.010±0.005	0.4±0.3	0.6±0.2	0.1±0.1	7.8±1.2	1.2±1.3
Charente	-	22.8±2.3	23.3±19.2	0.032±0.007	0.017±0.008	2.1±0.4	1.9±0.3	0.6±0.1	8.4±0.9	1.4±1.0
Adour	-	16.2±0.2	7.8±13.3	0.041±0.003	0.016±0.003	0.8±0.0	1.5±0.0	0.7±0.1	7.3±1.0	0.6±0.7

https://doi.org/10.5194/bg-2021-164
Preprint. Discussion started: 28 June 2021

Somme	-	28.7±2.2	21.5±24.3	0.014±0.005	0.018±0.009	0.9±0.3	1.1±0.3	0.4±0.2	9.0±0.9	4.7±1.2
Vilaine	-	23.2±3.2	17.2±14.4	0.024±0.011	0.045±0.028	1.9±0.7	1.5±0.4	1.9±0.3	8.7±1.0	4.5±1.6
Point source**										
Rouen WWTP	0.88	-	26.7	0.700	6.667	16.7	2	30.9	4.1	-
Nantes WWTP	1.35	-	26.7	0.700	6.667	16.7	2	30.9	4.1	-
Rochefort WWTP	0.11	-	26.7	0.700	6.667	16.7	2	30.9	4.1	-
Bordeaux WWTP	2.04	-	39.9	2.903	8.880	20	2	35.1	4.1	-
Bayonne WWTP	0.29	-	26.7	0.700	6.667	16.7	2	30.9	4.1	-

* The Dordogne River, which joins the Gironde estuary, is considered as an input to the estuary, in a way similar to the point sources, but with a daily time step (see Table 3), contrary to point sources** from WWTP inputs to the estuary for which we considered an annual average.

2.3.5. Simulation Set-Up

C-GEM simulates the transport and transformation in sequence by applying an operator splitting approach (Volta et al., 2014) and a finite difference scheme of a regular grid at 2 km with a time step of 150 s. The simulation starts following a 60-day warm-up during which only the hydrodynamics and transport terms are resolved, repeating the boundary constraints and forcings of the first tidal cycle, which enables the system to reach steady-state conditions. In this study, the model was run over a 3-year period from 2014 to 2016 for each estuary.

2.4. Model Calibration

The data used to calibrate and validate the model were obtained from the multiple databases mentioned in section 2.2. The locations of these stations along the estuaries are presented in Figure 1. Calibration was implemented based on 2015, an average year in terms of river discharge. The performance of the hydrodynamics modules was first evaluated by comparing the simulated salinity with observed salinity along the estuary. Then the mass transport was calibrated using longitudinal SPM profiles as an indicator. Good agreement with in situ data for salinity and SPM was reached by setting a maximum value of 100 m s^{-2} to the dispersion coefficient generated by the equations described in Volta et al. (2014). This dispersion value is in agreement with the previous study in the Scheldt estuary (Arndt et al., 2009) and the Loire estuary (Thouvenin et al., 1997). The values used for all parameters involved in the hydrodynamics and transport modules are presented in Table 5.

Table 5 Parameter settings related to salinity and sediment and their values along the estuaries (low, middle, and upstream parts).

Estuary	Settling velocity ($m\ s^{-1}$)	Chezy coefficient ($m^{0.5}\ s^{-1}$)			Erosion coefficient ($mg\ m^{-2}\ s^{-1}$)		Critical shear stress ($N\ m^{-2}$)	
		Low	Middle	Up	Low	Up	Low	Up
Seine	0.001	85	70	40	$1.6*10^{-5}$	$1.3*10^{-6}$	0.35	1.20
Loire	0.001	50	-	20	$5.0*10^{-5}$	$1.0*10^{-6}$	0.30	1.00
Gironde	0.001	80	40	35	$2.0*10^{-4}$	$8.8*10^{-6}$	0.30	1.00
Charente	0.001	50	-	20	$9.5*10^{-5}$	$8.0*10^{-6}$	0.25	1.00
Adour	0.001	40	-	20	$8.0*10^{-5}$	$5.0*10^{-6}$	0.30	0.80
Somme	0.001	50	-	30	$9.0*10^{-5}$	$2.0*10^{-7}$	0.35	1.20
Vilaine	0.001	30	-	20	$9.0*10^{-5}$	$8.0*10^{-6}$	0.30	1.20

Once the hydrodynamics were satisfactorily calibrated (see section 3.1), the biogeochemical module was calibrated using

https://doi.org/10.5194/bg-2021-164
Preprint. Discussion started: 28 June 2021

the observed water quality data, starting from the parameterization described in Laruelle et al. (2019a), which was used for an application of C-GEM to the Seine estuary. The same set of values for all biogeochemical parameters was used for all of the selected estuaries (Table 6), with only slight variation from the parameterization in Laruelle et al. (2019a) and ensuring that all parameters remained within a range corresponding to values representative of temperate estuaries following the extensive literature survey carried out by Volta et al. (2016a).

Table 6 Biogeochemical parameter values used in C-GEM.

Parameter name in C-GEM	Description	Unit	Value	Reference range (Volta et al., 2016a)
Pb[Phy]	Maximum specific photosynthetic rate	s^{-1}	$7.0*10^{-5}$	$1.07*10^{-6}$ ~ $1.82*10^{-4}$
alpha[Phy]	Photosynthetic efficiency	m^2 s $(\mu E*s)^{-1}$	$5.0*10^{-7}$	$1.67*10^{-7}$ ~ $6.94*10^{-7}$
kmortality[Phy]	Phytoplankton mortality rate constant	s^{-1}	$3.85*10^{-7}$	$2.3*10^{-7}$ ~ $2.35*10^{-5}$
kgrowth[Phy]	Phytoplankton growth constant	-	0.29	0.1 ~ 0.5
kmaint[Phy]	Phytoplankton maintenance rate constant	s^{-1}	$4.6*10^{-7}$	$1.6*10^{-7}$ ~ $3.5*10^{-6}$
kexcr[Phy]	Excretion constant	-	0.05	0.03 ~ 0.07
kbg	Background attenuation	m^{-1}	0.3	-
kspm	SPM attenuation	$(mg*m)^{-1}$	0.03	-
KPO_4	Michaelis–Menten constant for phosphate	µmol P	0.2	0.001 ~ 3.58
KN	Michaelis–Menten constant for dissolved nitrogen	µmol N	1.13	0.1 ~ 7.14
KNH_4	Michaelis–Menten constant for ammonium	µmol N	80	71.43 ~ 643.0
KNO_3	Michaelis–Menten constant for nitrate	µmol N	26.07	7.14 ~ 45.0
KDSi	Michaelis–Menten constant for dissolved silica	µmol Si	1.07	0.3 ~ 20.0
KTOC	Michaelis–Menten constant for organic carbon	µmol C	300	60 ~ 312.5
KO_2_ox	Michaelis–Menten constant for aerobic degradation	µmol O_2	31	15 ~ 34
KO_2_nit	Michaelis–Menten constant for nitrification	µmol O_2	51.25	15 ~ 312.5
$KinO_2$	Inhibition constant for nitrification	µmol O_2	33	15 ~ 63
Kox	Aerobic degradation rate constant	µmol C s^{-1}	$2.0*10^{-4}$	$9.75*10^{-5}$ ~ $9.26*10^{-4}$
Knit	Nitrification rate constant	µmol N s^{-1}	$5.0*10^{-4}$	$1.06*10^{-5}$ ~ $2.17*10^{-3}$
Kdenit	Denitrification rate constant	µmol N s^{-1}	$1.0*10^{-3}$	$2.6*10^{-5}$ ~ $5.22*10^{-1}$
pCO_2atmo	Current component for piston velocity	m s^{-1}	$3.9*10^{-4}$	-
redsi	Redfield ratio for silica	mol Si/mol C	15/106	-
redn	Redfield ratio for nitrogen	mol N/mol C	16/106	-
redp	Redfield ratio for phosphorous	mol P/mol C	1/106	-

After calibration of the hydrodynamic and biogeochemical processes for 2015, the model was then implemented and run for 2014 and 2016. The model validated over this longer time period using the parameterization constrained by the calibration over 2015. The results were evaluated against field measurements using widely used statistical indicators, namely, the root mean squared error (RMSE) and bias (Moriasi et al., 2007), which were calculated as:

$$\text{RMSE} = \sqrt{\sum_{i=1}^{n}(obs_i - sim_i)^2/n}$$

$$\text{Bias} = \sum_{i=1}^{n}(obs_i - sim_i)/\sum_{i=1}^{n} obs_i$$

where *n* is the number of samples, *obs* is the observation, and *sim* is the simulation. Evaluations are shown in section 3.1.

2.5. Calculation of Indicators of Estuarine Ecological Functions

To perform a year-long calculation of fluxes entering and leaving the estuarine system, the quantities transported through the boundaries of the system for each state variable were computed at each time step by the advection and dispersion schemes and integrated over the time period considered. This calculation and the relatively short computation time step of 150 s used

https://doi.org/10.5194/bg-2021-164
Preprint. Discussion started: 28 June 2021

by the model ensured accurate representation of the transient processes taking place during the tidal cycle in the estuary.

The retention rate of the estuary represents the intensity of the nutrient retention and/or elimination and/or transformations within the estuary and is calculated as:

$$\text{Retention Rate} = (\text{Flux}_{\text{in}} - \text{Flux}_{\text{out}})/\text{Flux}_{\text{in}} \times 100$$

where $Flux_{in}$ is the annual sum of all the inputs to any of the estuaries for dissolved inorganic phosphorus (DIP, which equals PO_4), dissolved inorganic nitrate (DIN, which equals NH_4 + NO_3), DSi, TOC; $Flux_{out}$ are the annual exports at the outlet of the estuaries.

The estuarine residence time was calculated considering the estuarine geomorphology and the river discharge to the estuary; therefore, it can be an indicator reflecting those two variables:

$$\text{Residence Time} = V/Q$$

where V is the estuarine volume (m^3) calculated by the integral from the estuarine length, width, and mean depth; Q ($m^3\ s^{-1}$) is the river mean annual discharge entering the estuary.

The indicator for coastal eutrophication potential (ICEP, Billen and Garnier, 2007; Garnier et al., 2010) allows quantifying estuarine nutrient flux balance or imbalance entering the coastal zone considering the excess of nitrogen (N) and phosphorus (P) to silica (Si), taking into account the N:P:Si stoichiometry according to the algae requirement. The ICEP is calculated as:

$$\text{P-ICEP} = [\ \text{Flux P}/31 - \text{Flux Si}/28 \times \text{P/Si}\ ] \times \text{C/P} \times 12$$

$$\text{N-ICEP} = [\ \text{Flux N}/14 - \text{Flux Si}/28) \times \text{N/Si}\ ] \times \text{C/N} \times 12$$

The P-ICEP and N-ICEP are expressed in carbon flux units (kg C km^{-2} d^{-1}), using the C:N and C:P Redfield ratios (Brzezinski, 1985; Redfield et al., 1963). Flux P, Flux N, and Flux Si are the mean specific fluxes of total phosphorus, total nitrogen, and dissolved silica, respectively, delivered at the outlet of the estuary, expressed in kg P km^{-2} d^{-1}, kg N km^{-2} d^{-1}, and kg Si km^{-2} d^{-1}.

3. Results

3.1. Model Performance

3.1.1. Calibration Based on 2015

The model was calibrated using available observations for the year 2015. The results from simulations performed using C-GEM and the corresponding observations were plotted for two dates in 2015 (one in winter [January] and the other in summer [July]) along the estuarine length for salinity, SPM, and water quality variables (PO_4, NH_4, NO_3, DSi, TOC, DO, Chl-a; Figure 3 and Figure S-1 in supplementary material, SM). The model was run using forcings and boundary conditions representative of the sampling dates of the field data.

The hydrodynamics module was calibrated on its ability to reproduce the salinity intrusion into the estuary under different conditions. Simulations followed the same increasing tendency with the measurements. In January, with high river

https://doi.org/10.5194/bg-2021-164
Preprint. Discussion started: 28 June 2021

discharges, the salinity intrusion reached 25 km from the sea mouth for large estuaries, such as the Seine and Loire estuaries, and within 50 km for the largest, the Gironde estuary. For the medium-size estuaries such as the Charente and Adour, salinity decreased to 1 at ~15 km from the sea mouth. During low discharges in July, salinity penetrated farther into the inner estuary, up to ~40–60 km from the sea mouth for large estuaries, while for the medium-size estuary it reached ~20 km from the sea mouth. Such seasonal and scale-dependent patterns for salinity agrees closely with observations.

Regarding SPM calibration, the model better captured the dynamics for the large estuaries than for smaller ones (Figure 3 and Figure S-1). Simulated SPM values were in the range of measured peaks, although some observations may be missing for the medium-size and small estuaries. The model generally provided an adequate representation of the turbidity maximum zone (TMZ). The Seine showed characteristics similar to the Loire, as they both showed a maximum SPM concentration at ~250 mg L^{-1} with TMZ quite close to the sea mouth (~20–30 km) in high discharge season and a maximum SPM concentration at ~500 mg L^{-1} with a TMZ up to ~40–50 km in low discharge season. The SPM of the Gironde ranged from ~1000 to ~2000 mg L^{-1} for the selected dates in 2015, with a TMZ located more upstream to the river, ~90–130 km to the sea mouth. Simulated SPM was low for the Charente, from ~70 mg L^{-1} in July to ~120 mg L^{-1} in January, and less than 10 mg L^{-1} for the Adour for both dates, but observations were very scarce.

Simulations of longitudinal variations in concentration for phosphates (PO_4), ammonium (NH_4), nitrate (NO_3), dissolved silica (DSi), and total organic carbon (TOC) for the two dates selected matched available observations. All nutrients, organic carbon, and Chl-a concentrations decreased mostly at the mouth, due to seawater dilution. In winter, high discharge led to increasing transport of elements (more than transformation), and longitudinal variations appeared rather flat. In summer, longitudinal profiles showed more transformation, e.g., within some estuaries an increase of PO_4 by desorption when salinity increased, before dilution at sea; development of phytoplankton also occurred within the estuaries, in the fluvial or saline sections (Figure 3).

PO_4 concentrations mostly varied within 0.1 mg P L^{-1} except for the Seine whose maximum concentration can reach 0.2 mg P L^{-1} in July with low discharge. Most observations were captured by the model, though at some stations the simulations overestimated the observations. NH_4 concentrations for the selected dates never exceeded 0.1 mg N L^{-1} except for the Adour at the first 15 km from the riverine boundary, with values varying from 0.1 to 0.15 mg N L^{-1}. NO_3 concentrations of the Seine, Loire, and Charente were higher (4–5 mg N L^{-1}) than the ones of the Gironde and Adour (~1.5–2.0 mg N L^{-1}). Simulated NO_3 underestimated the observations for the Loire in winter (in January at the ~ 30~70 km from the sea mouth), and slightly overestimated the NO_3 values for the Gironde at ~40–100 km from the sea mouth downstream of the confluence with the Dordogne tributary. DSi concentrations showed the highest concentrations for the Loire (7.0 mg Si L^{-1}), the lowest for the Charente and Adour (~2 mg Si L^{-1}), and intermediate for the Seine and Gironde (~5 mg Si L^{-1}). Regarding the TOC level, they were on the order of 5 mg C L^{-1} for these five estuaries: slightly lower in summer, except for the Seine (Figure 3).

For each variable, the fit between simulations and observations was evaluated through the value of Bias and RMSE (Table 7).

https://doi.org/10.5194/bg-2021-164
Preprint. Discussion started: 28 June 2021

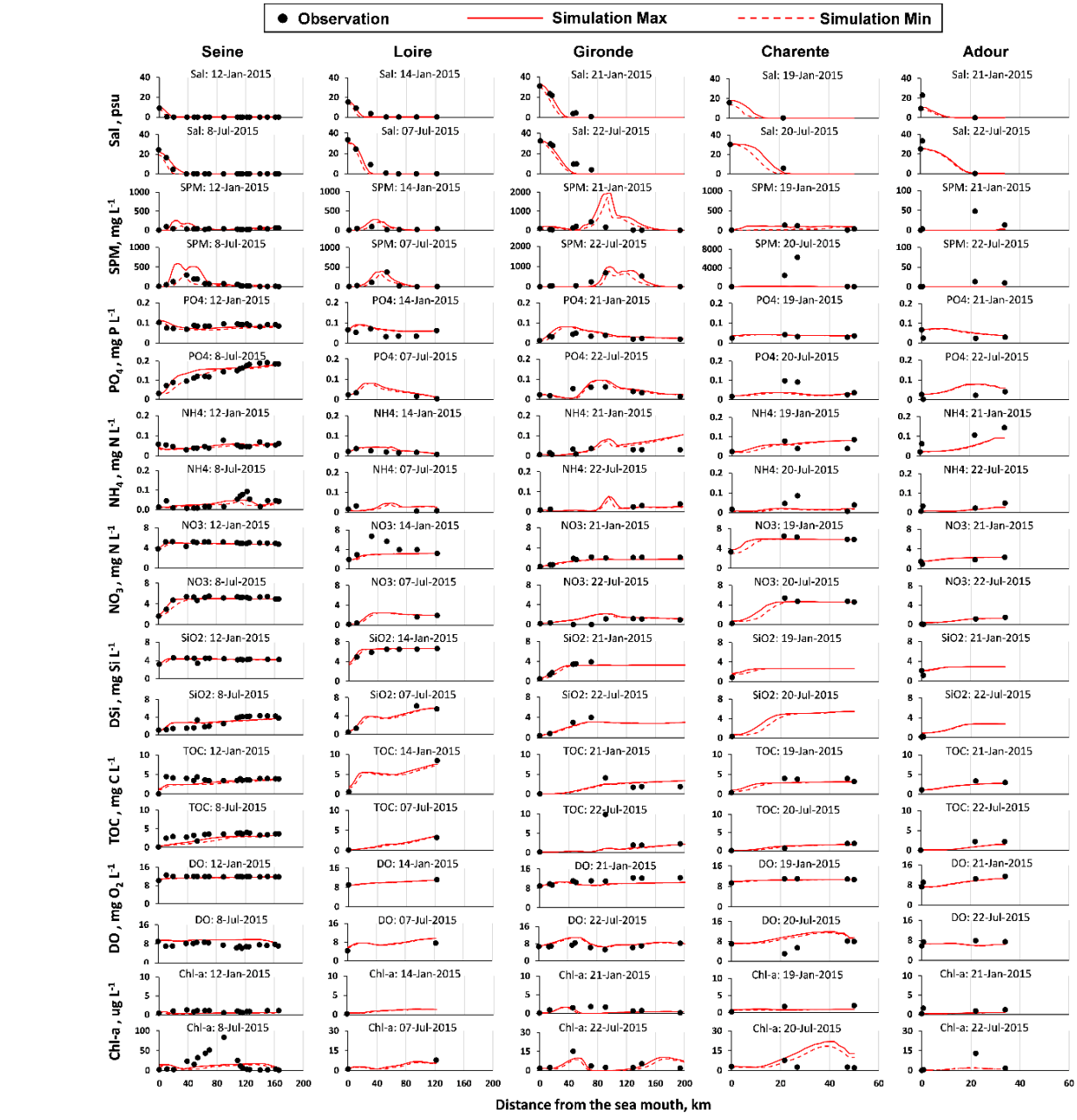

Figure 3 Salinity (Sal), suspended particulate matter (SPM), and nutrients (PO_4, NH_4, NO_3, DSi, TOC), dissolved oxygen (DO), chlorophyll a (Chl-a) concentration variations along the estuaries (the Seine, Loire, Gironde, Charente, and Adour) for two selected dates (one in winter and the other one in summer). Note the different scales for the SPM and Chl-a for the estuaries. The results of the Somme and Vilaine estuaries are shown in the supplementary material.

These comparisons show that the model provides simulations in agreement with the available observations; the statistical indicators (Table 7) also confirmed the satisfactory performance of the model through the standards provided by Moriasi et al. (2007, $-0.7 < \text{Bias} < 0.7$). The RMSEs were consistent in both calibration and validation periods, remaining within the

https://doi.org/10.5194/bg-2021-164
Preprint. Discussion started: 28 June 2021

range of standard deviation values provided in Table 4 for upstream boundary conditions.

Table 7 Bias and root mean square error (RMSE) for salinity (Sal), phosphate (PO_4), ammonia (NH_4), nitrate (NO_3), dissolved silica (DSi), total organic carbon (TOC) for the Seine, Loire, Gironde, Charente, Adour, Somme, and Vilaine estuaries.

Variables	Unit	Estuary	Calibration			Validation		
			n	Bias	RMSE	n	Bias	RMSE
Sal	psu	Seine	132	−0.29	0.68	266	−0.17	1.34
		Loire	60	0.30	4.83	120	0.39	4.05
		Gironde	34	0.41	5.62	62	0.40	5.11
		Charente	0	-	-	2	NR*	NR*
		Adour	12	0.34	11.05	26	0.21	8.86
		Somme	24	0.11	2.79	51	0.11	3.44
		Vilaine	24	0.15	6.87	48	0.12	7.04
PO_4	mgP L^{-1}	Seine	150	0.01	0.02	299	−0.03	0.02
		Loire	34	−0.42	0.03	70	−0.35	0.02
		Gironde	72	0.00	0.02	141	−0.21	0.03
		Charente	24	0.21	0.03	46	0.29	0.07
		Adour	24	−1.16	0.03	48	−0.44	0.03
		Somme	24	0.00	0.01	53	0.02	0.01
		Vilaine	24	0.28	0.02	48	0.22	0.02
NH_4	mgN L^{-1}	Seine	150	0.04	0.13	299	0.16	0.07
		Loire	34	−0.20	0.02	70	0.13	0.02
		Gironde	72	0.85	0.62	141	0.78	0.35
		Charente	24	0.24	0.03	46	0.54	0.12
		Adour	24	0.65	0.06	48	0.71	0.21
		Somme	24	−0.01	0.01	53	0.18	0.03
		Vilaine	24	0.29	0.04	48	0.50	0.08
NO_3	mgN L^{-1}	Seine	150	0.06	0.70	298	0.05	0.55
		Loire	34	0.20	1.08	70	0.15	0.67
		Gironde	72	0.15	0.47	141	0.07	0.33
		Charente	24	0.08	0.51	46	0.05	0.51
		Adour	24	−0.09	0.48	48	0.01	0.46
		Somme	24	−0.21	0.54	53	−0.22	0.61
		Vilaine	24	−0.23	1.02	48	−0.32	0.96
DSi	mgSi L^{-1}	Seine	132	0.10	0.69	269	0.11	0.66
		Loire	34	−0.08	1.33	70	−0.08	0.88
		Gironde	36	0.22	1.60	103	0.15	1.10
		Charente	0	-	-	2	NR*	NR*
		Adour	14	−0.43	0.95	26	−0.16	0.74
		Somme	24	−0.19	0.83	51	−0.20	0.88
		Vilaine	24	−0.19	0.47	48	−0.15	0.63
TOC	mgC L^{-1}	Seine	150	0.27	1.17	299	0.26	1.51
		Loire	0	-	-	0	-	-
		Gironde	42	0.27	1.67	90	0.25	1.20
		Charente	24	0.35	2.77	46	0.18	1.08
		Adour	12	0.39	1.11	24	0.39	1.22
		Somme	11	−0.06	0.23	24	0.01	0.22
		Vilaine	0	-	-	0	-	-

* NR, not relevant in the case of a data set with fewer than 10 samples.

3.1.2. Validation for 2014 and 2016

After the calibration performed on the year 2015, the model was implemented over the entire 2014–2016 period for

https://doi.org/10.5194/bg-2021-164
Preprint. Discussion started: 28 June 2021

validation. Figure 4 shows the performance of the C-GEM model over the entire period studied (from 2014 to 2016, including the calibration and validation periods). The seasonal variations are depicted here at specific monitoring stations located in the lower part of each estuary (but not too close to the marine boundary conditions in order to capture the dynamics of the model and minimize the influence of the marine boundary; note that the validation results of the small-scale estuaries are presented in Figure S-2 in the SM). A rather good evaluation of these water quality time series simulations is confirmed by the Bias and RMSE indicators (Table 7).

In agreement with the longitudinal profiles simulated for the calibration period (Figure 3), the seasonal PO_4 levels (simulated and observed) in the downstream Seine estuary (average, 0.11 mg P L^{-1}) was twice as large as those for the other estuaries (ranging on average from 0.04~0.07 mg P L^{-1}). Similar to PO_4, NH_4 mostly came from discharged wastewater not completely treated in WWTPs and also showed the highest levels in the Seine estuary, with large variations (0.01–0.35 mg N L^{-1}). Similar large magnitudes for NH_4 concentrations were also found for the medium-size and small estuaries (Figure 4).

The NO_3 concentrations of the Seine (4.8 mg N L^{-1}), the Charente (5.3 mg N L^{-1}), and the Somme (4.7 mg N L^{-1}) were ~2–4 times higher than the Loire (2.6 mg N L^{-1}), Gironde (1.6 mg N L^{-1}), Adour (1.4 mg N L^{-1}), and Vilaine (2.3 mg N L^{-1}); the DSi values of the Somme (9.0 mg Si L^{-1}), Loire (5.1 mg Si L^{-1}), and Charente (4.8 mg Si L^{-1}) were ~1.4–3.3 times larger than in the other systems (2.7~3.5 mg Si L^{-1}, Figure 4). The simulations of TOC in the Loire (3.7 mg C L^{-1}) and Vilaine (2.8 mg C L^{-1}) appeared larger than in the other systems, but no measured TOC values were available; TOC simulation levels in the Seine (2.3 mg C L^{-1}), Charente (1.9 mg C L^{-1}), Adour (1.5 mg C L^{-1}), and Somme (2.6 mg C L^{-1}) were in agreement with the observations. As shown by the highest algal biomass (Chl-a peaked to 40–50 µg L^{-1}), the Seine estuary was the most eutrophic system (Figure 4). All the estuaries studied seemed well-oxygenated during the study period (2014–2016). DO varied around the same range, with mean values from 8.0 to 9.9 mg O_2 L^{-1}, but for the Charente, DO dropped to <5.0 mg O_2 L^{-1} during July–September, which was not well represented by the model (Figure 4).

In addition, seasonal trends are properly captured for nutrient, DO, and Chl-a concentrations. PO_4 values were higher in summer when low river discharge diluting effluent discharged from WWTPs was lower, while this trend was not as clear for NH_4, even though it also came from wastewater effluents. The NO_3 concentration clearly showed a seasonal decrease from winter to autumn for most of the estuaries studied (Figure 4). DSi concentrations indicated lower values mostly in spring and late summer, necessarily linked to diatom uptake, which corresponded to Chl-a peaks, clearly visible in the Seine, Somme, and Vilaine. The simulation underestimated silica uptake in 2014 for the Gironde. For the other estuaries, seasonal DSi patterns were not clear and data were often missing. The highest TOC level occurred in winter, with higher discharges and high SPM, although some high summer values can be linked to biological biomass. DO showed a regular trend with high values in winter and low values in summer, according to its solubility, but also to its consumption with high summer mineralization (cf. the Charente, especially in Figure 4). Conversely, phytoplankton growth might episodically enhance oxygen, as shown by the short-term peak of the model, even though the excessively scarce data cannot support the pattern at such a time scale.

https://doi.org/10.5194/bg-2021-164
Preprint. Discussion started: 28 June 2021

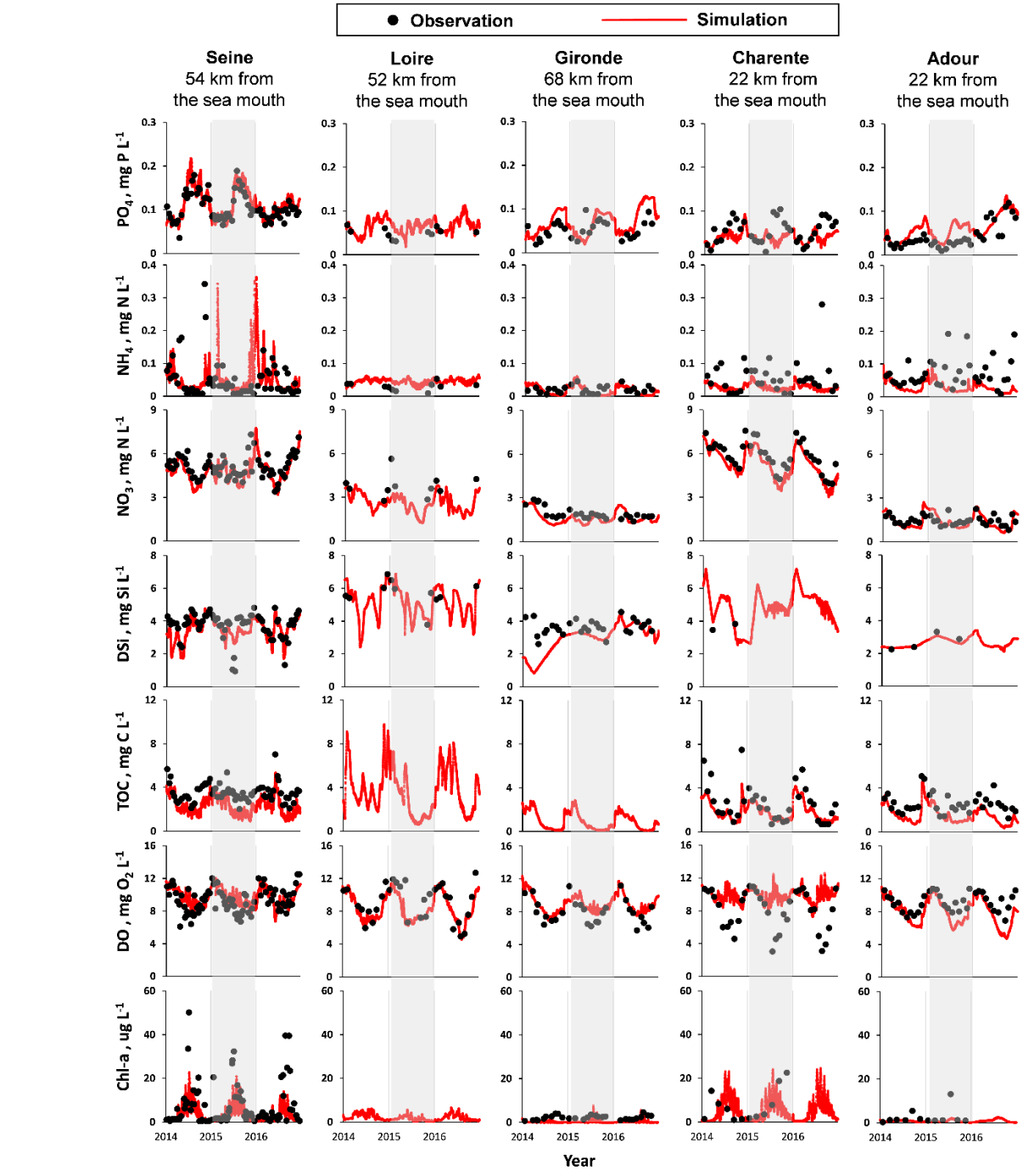

Figure 4 Temporal variations for phosphate (PO_4), ammonium (NH_4), nitrate (NO_3), dissolved silica (DSi), total organic carbon (TOC), dissolved oxygen (DO), and chlorophyll a (Chl-a) concentrations from 2014 to 2016 for the Seine, Loire, Gironde, Charente, and Adour estuaries at the sampling stations located about 1/3 the length of the estuary to the sea mouth. Gray columns covered the year of calibration (2015). The results of the Somme and Vilaine are shown in the supplementary material.

https://doi.org/10.5194/bg-2021-164
Preprint. Discussion started: 28 June 2021

3.2. Biogeochemical Budgets

3.2.1. Ingoing and Outgoing Fluxes

Considering the suitable agreement between simulations and observations, a reasonable level of confidence can be attributed to the ingoing and outgoing nutrient fluxes calculated by the model at the limits of the estuaries, e.g., dissolved inorganic nitrogen (DIN=NH_4+NO_3), dissolved inorganic phosphorus (DIP=PO_4), dissolved silica (DSi), Phy (Chl-a, using a C/Chl-a ratio of 40 (Jakobsen and Markager, 2016)), and TOC were calculated (Table 8). In addition, the Redfield–Brzezinkski ratio C:N:P:Si = 106:16:1:15–20 (Brzezinski, 1985; Redfield et al., 1963) was used to take into account the organic fractions and estimate total nitrogen (TN), total phosphorus (TP), and total silica (TSi), whose fluxes were preferentially chosen for calculating overall retention rates (see section 3.2.2).

The import of TN ranged from 5.46 (Somme) to 104.58 kt N yr^{-1} (Loire), TP from 0.10 (Somme) to 4.97 kt P yr^{-1} (Loire), TSi from 9.39 (Somme) to 141.94 kt Si yr^{-1} (Loire), Phy from 0.07 (Somme) to 3.11 kt C yr^{-1} (Loire), and TOC from 2.78 (Somme) to 154.88 (Loire) kt C yr^{-1}. Although the river discharge of the Gironde estuary was slightly larger (2%) than that of the Loire, the Loire estuary received larger nutrient fluxes (1.7 times for TN, 2.6 times for TP, 15.3 times for TSi, 2.4 times for Phy, and 2.0 times for TOC) than the Gironde. Further, the Loire, with 1.6 times the discharge of the Seine estuary, imported only 1.2 times the TN flux to its estuary but 1.8 times the TP flux. The river discharge of the Adour was quite similar to the Seine (86% of the Seine), but its TN, TP, TSi, Phy, and TOC imports amounted to only 25%, 34%, 47%, 24%, and 40%, respectively, of those of the Seine (Table 8).

Based on this study, around 259 kt N yr^{-1} of TN, 9.6 kt P yr^{-1} of TP, 304 kt Si yr^{-1} of TSi, and 145 kt C yr^{-1} of TOC were exported to the French Atlantic Ocean through these seven estuaries. They accounted for about 80% of the total water discharge from all the estuaries on the French Atlantic coast (based on long-term analysis of runoff data from French national databases) and 83% of the total watershed areas on the French Atlantic coast, and hence a similar proportion of the nutrient fluxes.

Table 8 The mean annual (2014–2016) import and export of nutrients (total nitrate (TN), total phosphorous (TP), total silicate (TSi), phytoplankton (Phy), and total organic carbon (TOC)) for the estuaries studied.

Variables		Unit	Estuary						
			Large-scale			Medium-scale		Small-scale	
			Seine	Loire	Gironde	Charente	Adour	Somme	Vilaine
Annual mean Q		$m^3\ s^{-1}$	499	808	824	77	431	48	96
Riverine basin area		km^2	65,000	111,436	51,343	7598	14,832	5560	10,498
Estuarine basin area		km^2	11,843	6891	31,459	2327	2122	820	237
Whole basin area		km^2	76,843	118,327	82,802	9925	16,954	6380	10,735
Estuarine residence time		day	16	20	79	12	2	17	8
Export	TN	kt N yr^{-1}	78.52	68.96	46.47	13.89	19.07	5.39	26.74
	TP	kt P yr^{-1}	2.28	3.88	1.35	0.21	0.93	0.1	0.87
	TSi	kt Si yr^{-1}	52.34	133.22	56.24	11.54	25.98	8.85	16.02
	Phy	kt C yr^{-1}	11.63	3.56	1.91	0.13	0.19	0.37	1.17
	TOC	kt C yr^{-1}	25.14	63.99	3.44	4.81	16.02	2.45	29.79
Import	TN	kt N yr^{-1}	84.9	104.58	61.38	14.75	21.29	5.46	26.18
	TP	kt P yr^{-1}	2.8	4.97	1.9	0.23	0.94	0.10	0.92
	TSi	kt Si yr^{-1}	55.97	141.94	90.27	12.04	26.44	9.39	16.07

https://doi.org/10.5194/bg-2021-164
Preprint. Discussion started: 28 June 2021

Phy	kt C yr^{-1}	0.96	3.11	1.29	0.14	0.23	0.07	1.15
TOC	kt C yr^{-1}	56.73	154.88	75.87	6.75	22.54	2.78	31.54

Note:
DIN=NH_4+NO_3, TN=DIN+(Phy (in C)+TOC)/5.7 (the Redfield–Brzezinkski ratio, Brzezinski, 1985; Redfield et al., 1963)
DIP=PO_4, TP=DIP+(Phy (in C)+TOC)/41 (the Redfield–Brzezinkski ratio, Brzezinski, 1985; Redfield et al., 1963)
TSi=DSi+Phy (in C)/2.8 (the Redfield–Brzezinkski ratio, Brzezinski, 1985; Redfield et al., 1963)

Interestingly, considering the specific TP, TN, and TOC fluxes to the estuaries (i.e., total influxes per surface area of river basin) makes it possible to infer the contamination in the watersheds. The Vilaine and the Charente estuaries receive the highest fluxes of TN, while the Vilaine and Adour estuaries were the receptacles for greater TP fluxes, the Loire and Gironde estuaries for TOC fluxes (Figure 5). Although silica is a major nutrient for diatom algae populations, differently from anthropogenic N and P sources, it is of natural origin (rock weathering) and reveals the lithology of the watershed, with higher fluxes for the Gironde and Adour estuaries (Figure 5). Overall TN specific fluxes exceeded 900 kg N km^{-2} yr^{-1}, varying within a range of 2.5 times, and TSi specific fluxes exceeded 850 kg Si km^{-2} yr^{-1}, varying within a range of 2.1 times, while TP and TOC specific fluxes were more variable, within a factor close to 5~6 (Figure 5).

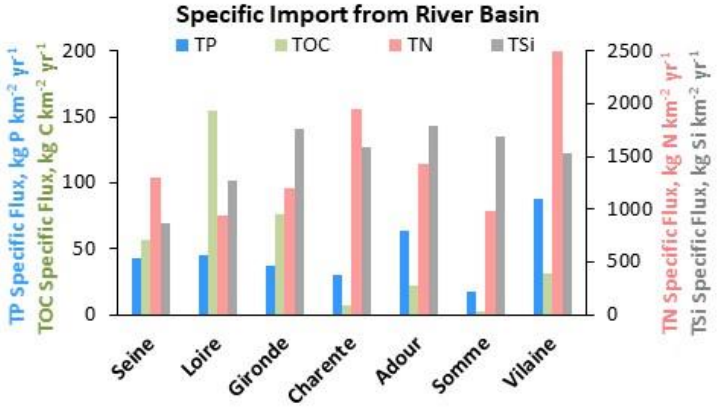

Figure 5 Average annual (2014–2016) specific fluxes of total phosphorus (TP), nitrogen (TN), organic carbon (TOC), and silica (TSi) entering the estuaries studied.

3.2.2. Retention Rate

To determine the different ecological functions of the estuaries studied, their retention rates for TN, TP, TSi, and TOC were quantified following the equations presented in section 2.4 (Figure 6).

For the large estuaries (the Seine, Loire, and Gironde), the retention rate for TN ranged from 8% to 34%, for TP from 19% to 27%, for TSi from 6% to 39%, for TOC from 56% to 96%. For the medium-size estuaries (the Charente and Adour), the retention rate was 7–10% for TN, 1–12% for TP, 2–7% for TSi, and 30–32% for TOC. For the small estuaries (length <20 km, the Somme and Vilaine), the retention rate for TN, TP, TSi, and TOC were 0–1%, 0–7%, 2–6%, and 8–12%, respectively.

The Loire estuary showed the largest retention rate for TN; the Gironde estuary is the most retentive for TP, TSi, and TOC.

https://doi.org/10.5194/bg-2021-164
Preprint. Discussion started: 28 June 2021

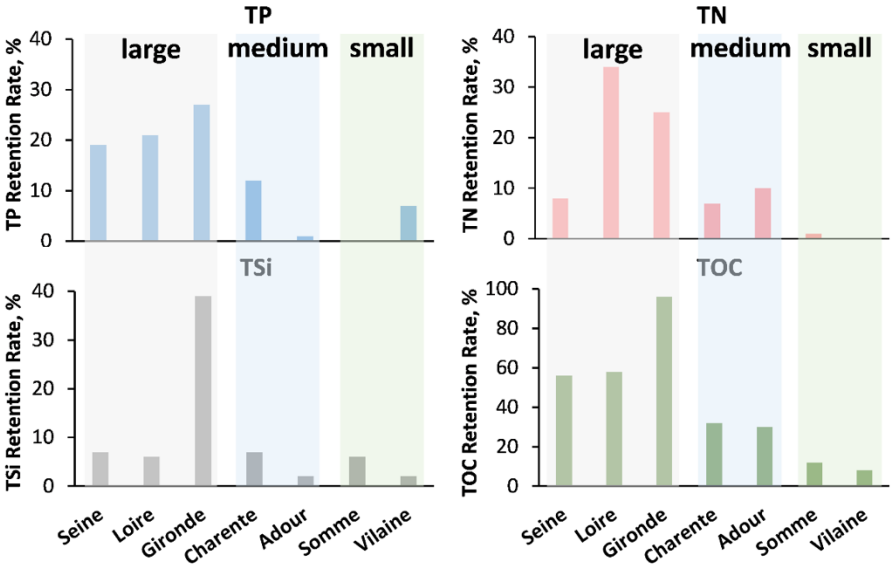

Figure 6 Annual mean (2014–2016) retention rates for the seven estuaries studied in terms of total phosphorus (TP), nitrogen (TN), organic carbon (TOC), and silica (TSi).

For the three large estuaries, the annual mean residence time was around 14–27 days for the Seine and Loire, but longer for the Gironde estuary: 70–97 days. Longer residence time indeed causes higher retention rates for the Gironde (Figure 6 and Figure 7). For the two medium-size estuaries, the residence time differed substantially: for the Charente, it ranged from 9 to 18 days while the residence time of the Adour was only 2–3 days during the study period. The Adour estuary had a shorter estuarine length and was narrower but with an approximately six times greater river discharge compared to the Charente. Thus, the retention rate for the Charente estuary was also higher (Figure 6 and Figure 7). Small estuaries such as the Somme and Vilaine had a residence time ranging from 5 to 18 days. The Vilaine had a short estuarine length due to the dam located 10 km from the sea mouth. Therefore, the residence time of the Vilaine estuary depends on the dam's regulation and the residence time of the dam/reservoir at the interface of the river outlet and the estuary (Figure 6 and Figure 7). Most of the retention may therefore occur in the dam reservoir, thus favoring nutrient uptake by phytoplankton and loss of N via denitrification (Garnier et al., 1999; Seitzinger et al., 2006; Yan et al., 2021) and in total reducing estuarine retention itself.

We therefore plotted the relationship between annual retention rates for water quality variables (TN, TP, TSi, and TOC) and annual mean residence time for 2014–2016 for each estuary studied (Figure 7). The retention rates for TSi and TOC showed a significant positive relationship (R^2=~0.6, $p<0.05$, Figure 7) with annual mean residence time, while the positive relationship was less clear for TN and TP retention rates.

https://doi.org/10.5194/bg-2021-164
Preprint. Discussion started: 28 June 2021

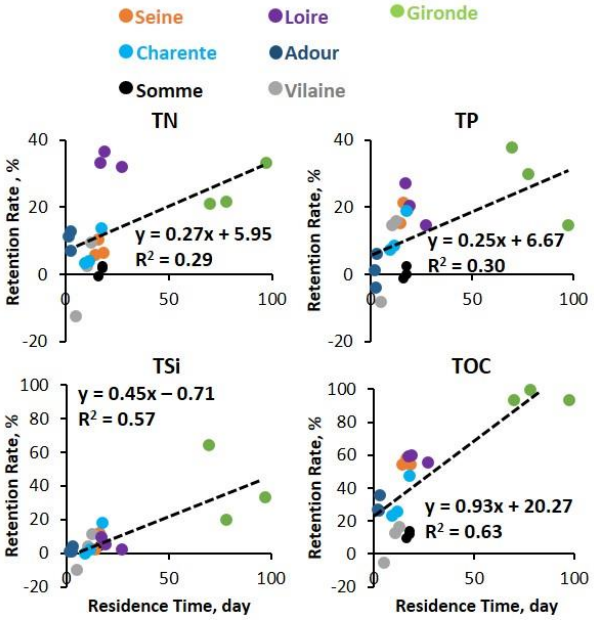

Figure 7 The relations between the annual retention rate for nutrients (total nitrogen (TN), total phosphorus (TP), total silica (TSi), and total organic carbon (TOC)) and the annual mean residence time for the estuaries studied (the Somme, Seine, Vilaine, Loire, Charente, Gironde, and Adour estuaries) for the 3 years 2014–2016.

3.3. The Indicator of Coastal Eutrophication Potential

The ICEP was calculated on the basis of estuarine TN, TP, and TSi deliveries (Figure 8). The N-ICEP values at the sea mouth were all positive and ranged from 2.1 (Loire) to 14.5 kg C km^{-2} d^{-1} (Charente), while the P-ICEPs at the sea mouth were all negative, ranging from −8.7 (Adour) to −3.8 kg C km^{-2} d^{-1} (Seine). The N-ICEPs were positive and the P-ICEPs were negative for all the estuaries studied, indicating that TN was in excess relative to TSi, revealing a risk of coastal eutrophication and the development of potentially harmful nonsiliceous algae. Regarding the P-ICEP, the systematic negative values would rule out any risk of eutrophication, although the P-ICEP closest to zero for the Seine and the Gironde would indicate that these systems are fragile, given that increased P in case of low discharge could become positive and lead to eutrophication.

Referring to the potential of coastal marine eutrophication, we calculated the P- and N-ICEP at the entrance and outlet of the estuary, to determine the buffer role of estuaries regarding eutrophication potential (Figure 8). Whereas the P-ICEP was less negative at the outlet compared to the inlet, the N-ICEP was generally lower at the outlet, meaning that there was a lower deficit in phosphorus compared to silica, and a reduced excess in nitrogen, except for the Vilaine for which both the P- and N-ICEPs are similar.

https://doi.org/10.5194/bg-2021-164
Preprint. Discussion started: 28 June 2021

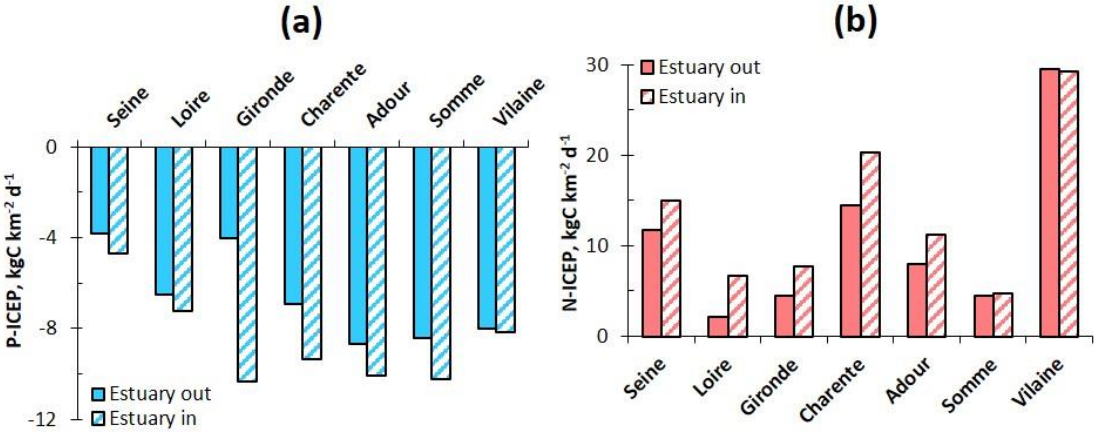

Figure 8 Indicator of costal eutrophication potential (ICEP, (a): P-ICEP; (b): N-ICEP) for the estuaries studied.

4. Discussion

4.1. Model Applicability and Limitations

The 1-D biogeochemical model C-GEM was built to overcome the requirement of large, often unavailable data sets of complex multidimensional models and to improve computation efficiency and consequently enable regional- and/or global-scale applications using a generic, theoretical framework based on the direct relationship between estuarine geometry and hydrodynamics (Volta et al., 2014, 2016b). As mentioned above, this requires easily obtainable geometrical parameters to frame the idealized morphology of the estuary and uses a set of exponential functions to estimate the width profile of the channel and the cross-section variations along the longitudinal axis. The sensitivity of biogeochemical processes to uncertainties in parameter values provided by Volta et al. (2014a) revealed on large estuaries that the convergence length and water depth had an important influence on the biogeochemical functioning of the estuary due to their strong constraint over the hydrodynamics and transport of solids within the system (Savenije, 2012). We could thus expect a less satisfactory performance on small-scale estuaries (Somme and Vilaine, Table 7, Figure S-1 and Figure S-2 in the SM) than on medium- and large-scale estuaries. Indeed, the spatial resolution used in C-GEM is 2 km, which allows capturing the dominant features of large estuaries while it can be too coarse for small estuaries (length <30 km) of this study. For future applications on small estuaries, the grid size might need to be adjusted.

C-GEM considers essential biogeochemical processes and reactions, though few potentially important processes, such as benthic–pelagic exchanges, sorption–desorption of phosphorous, and mineral precipitation, a more complex representation of the biological planktonic/benthic compartments (such as grazing by higher trophic levels, or multiple reactive organic carbon pools), are not included (Laruelle et al., 2017). In the present study, a simple representation of particulate matter burial was nonetheless implemented and applied to phytoplankton and TOC to provide a first-order representation of the process, which is necessary to evaluate the retention of carbon and nutrients within the system. Indeed, the only other

https://doi.org/10.5194/bg-2021-164
Preprint. Discussion started: 28 June 2021

potential nutrient removal term is denitrification for nitrogen.

In addition to the idealized geometry and biogeochemical processes, the boundary conditions and constraints are also critical for the performance of the model because they place the simulated system in an environmental context and drive transient dynamics. In this study, marine boundary conditions were extracted from ECO-MARS3D (Cugier et al., 2005b; Lazure and Dumas, 2008; Ménesguen et al., 2019), and are thus model-derived. Consequently, the results depend on the robustness of the ECO-MARS3D predictions, which is better for hydrodynamic variables (elevation, temperature, salinity, currents) than for biogeochemical variables. Riverine boundary conditions comprise the observed data, extracted at the station closest to the model's upper boundary, which might still be located several kilometers upstream or downstream of the model's upstream boundary. Observed data are usually measured at monthly or bimonthly intervals. Some variables were sampled more frequently, two or three times per month, while Chl-a concentrations were usually only available from March to September. Also, DSi, TOC, and Chl-a are usually less available than other variables. Instantaneous SPM and water quality sampling data were linearly interpolated to obtain the daily values between the adjacent measurements. Therefore, simulations are only partly transient and do not resolve events such as storms, floods, and/or extreme droughts.

In this study, only WWTPs from the largest estuarine cities (>50,000 inhabitants) were considered in the estuarine model. The volume of water released by WWTPs to the estuaries may change over a year, especially in the touristic estuarine cities in summer. However, even if the summer fluxes double and the summer river discharges decrease by half compared to the average values, wastewater discharge would remain below 3% of the total.

Although these simplifications and limitations, e.g., morphological and boundary inputs, C-GEM captured the main spatial and seasonal trends, also considering potential inaccuracies from the sampling strategy (surface sampling, ebb or flow, etc.). Its performance is supported by simulation/observation comparisons with longitudinal profiles from specific days (Figure 3 and Figure S-1 in the SM), and/or simulation/observation comparisons at specific cross sections (Figure 4 and Figure S-2), and/or evaluation analysis (Table 7). Moreover, the performance of C-GEM has been tested on other systems – carbon processing in the six major tidal estuaries (length >80 km) flowing into the North Sea (Volta et al., 2016b), biogeochemical dynamics and CO_2 exchange in three tidal estuaries (length >90 km, Volta et al. 2016a), CO_2 evasion on 42 tidal estuaries along the US east coast (Laruelle et al., 2017) and the Seine (Laruelle et al., 2019), biogeochemical processes and fluxes on a tropical estuary (Nguyen et al., 2021) – and solid results were gained. The implementations on different sized estuaries in this study confirmed that this model is not only applicable to large estuaries but also to smaller ones (length <50 km).

4.2. Fluxes and Retention Capacity

Quantifying fluxes (section 3.2.1) showed that even though some estuaries received nearly the same water flow from the upstream basin, their nutrient imports can differ greatly, due to the range of the human population and land use in the upstream watersheds. This is illustrated, for example by the Seine and Loire compared with the Adour. Anthropogenic influences have been recognized as an important factor affecting water quality as well as nutrient fluxes not only in rivers from headwater to downstream estuarine and coastal waters, but also in stagnant systems (Baker, 2005; Escolano et al., 2018;

https://doi.org/10.5194/bg-2021-164
Preprint. Discussion started: 28 June 2021

Garnier et al., 2019; Nguyen et al., 2021). In this study, the basins are characterized by different land use types. For example, the Somme, Seine, Vilaine, and Charente basins are dominated by intensive agriculture with arable land covering 66–84% of the total basin area (Table 2). Moreover, the Seine, Loire and Gironde basins have a population ranging from 4.91 to 16.7 M inhabitants. The population in the Seine basin is even 2 and ~3.4 times larger than that of the Loire and Gironde, respectively. The positive relationship between retention rates and residence time confirms that estuarine geomorphology and river fluxes are major physical forcings for biogeochemical retention abilities (Arndt et al., 2009; Perez et al., 2011; Romero et al., 2019). This relationship between estuarine residence time and retention capacity was already theorized empirically on a handful of systems in the pioneering work of Nixon et al. (1996). While deriving a predictive formula for nutrient retention solely based on geometric parameters and nutrient loads remains elusive (Laruelle, 2017), this study presents further evidence of the importance of water residence time in the complex interplay of physical and biogeochemical drivers constraining the retention potential of a given estuarine system.

The retention rates for TSi and TOC showed relatively significant positive relationships (Figure 7) with annual mean residence time, while relationships between TN and TP retention rates and the annual mean residence time were weaker. This can be caused by anthropogenic interferences with the biogeochemical processes within the estuaries. For example, the high retention for TN in the Loire estuary might be due to an elimination process in this system. For the Vilaine basin, 2014 was a wet year with a discharge double those recorded in 2015 and 2016, leading to slightly negative retention rates, meaning that instead of eliminating nutrients, the Vilaine estuary exported a small amount (Figure 7). The export of nutrients likely corresponds to a difference in the nutrient stock within the system itself between the beginning and the end of the simulated period and remains limited to a few percent of the riverine loads.

The retention rates were also compared with other estuaries. A yearly retention rate of 6.8–13% for TN, 27–31% for TP, and 4.3–11% for DSi were found for the Seine estuary (Garnier et al., 2010b; Romero et al., 2019), while we found here, for the 2014–2016 period, values of 6–10% for TN, 15–21% for TP, and 2–12% for TSi, which agree closely with the earlier studies. For tidal estuaries discharging into the North Sea, a15% retention rate for total C was found (Volta et al., 2016b), and the Scheldt estuary showed a 73% and 78% reduction of NH_4 and TOC, respectively (Vanderborght et al., 2007), and a retention rate of 12% for DSi and 32% for TN. Seitzinger (1988) found a 20–50% elimination of N for six estuaries, while for a tropical system, Luu et al. (2012) mentioned a 43.6%retention rate for N. Interestingly, the retention rates for individual systems are highly variable (Arndt et al., 2009). Here, TOC retention rates varied greatly among different systems, from 10% (the Somme estuary in 2014) to 100% (the Gironde estuary in 2016). With the longest residence time and the high level of suspended matter and associated TOC, the Gironde is a site for high TOC retention, as already shown by Etcheber et al. (2007). TN filter capacities ranged from 0% (the Somme estuary in 2014) to 37% (the Gironde estuary in 2016), due to denitrification and burial. TSi was eliminated only slightly (e.g., 2% for the Seine estuary in 2016 and the Loire in 2015 and 1% for the Adour in 2014 and 2015), meaning that no diatom uptake occurred or was compensated by diatom outburst under osmotic pressure (Ragueneau et al., 2002; Roubeix et al., 2008). High DSi retention in the Gironde (39%) may be linked to detrital particle removal by burial. With high suspended matter and low light penetration, turbid estuaries showed low

https://doi.org/10.5194/bg-2021-164
Preprint. Discussion started: 28 June 2021

diatom planktonic primary production (Coynel et al., 2005).

4.3. Coastal Eutrophication Potential

Eutrophication has been recognized as a serious environmental threat for both rivers and marine waters. The amount of nutrients (N, P, Si) delivered to the coastal zone by large river systems are the major determinants of coastal marine eutrophication problems. Previous studies have indicated that eutrophication is not only a result of high inputs of anthropogenic nutrients (N and/or P), but also of the imbalance when anthropogenic N and P are introduced over Si from natural rock weathering (Billen and Garnier, 1997; Garnier et al., 2021). Therefore, the ICEP considers the balance of these nutrients (N, P, Si) to calculate the coastal eutrophication potential in watershed area units (kg C km^{-2} day^{-1}) for comparisons between the P- and N-ICEP (C unit) and among systems (per km^2).

The P-ICEPs were all negative while the N-ICEPs were all positive for the estuaries studied herein, indicating a deficit in P and excess N, respectively, with respect to the Si requirements of diatoms (Billen and Garnier, 2007). The negative values for the P-ICEP for small to medium-size estuaries are larger than for large-scale estuaries (Figure 8). Accordingly, there would be no risk for potential coastal eutrophication regarding P; however, the rapid cycling of this element in coastal marine systems generally prevents it from becoming limiting (Kobori and Taga, 1979; Labry et al., 2016). Conversely, positive N-ICEP values might be responsible for the eutrophication problems observed and did not relate to estuary size. While exploring the N-ICEP over the long term (from 1950 to the 2010s), Garnier et al. (2010a) found an increase as a function of population density and rapid urbanization leading to the development of sewerage systems without sufficient treatment of sewage water, and also with rapidly increasing agricultural production.

The manifestations of eutrophication along the coast are diverse. *Phaeocystis* blooms have been reported in the Somme Bight (Lamy et al., 2006; Lefebvre et al., 2011), while *Dinophysis* (dinoflagellates) and *Pseudo-nitzschia* (diatoms) are the dominant harmful algae in the Seine Bight (Cugier et al., 2005a; Garnier et al., 2019; Ménesguen et al., 2019). Whereas most of the rivers have shown a decrease in phosphorus in the last two decades (Romero et al., 2013), leading to a negative P-ICEP, as found here, algal biomass increased (diatoms and dinoflagellates) with a shift in the peak in the Vilaine Bight (Ratmaya et al., 2019), mostly due to N fluxes brought by the Loire River, which flows northwards with the currents (Ménesguen et al., 2018a, 2019) and to internal sources from sediments (Ratmaya et al., 2019). No strong eutrophication problems have been reported off the Loire estuary, in the North Biscay Bay, without major changes during the last two decades, in contrast to the North of France (Gohin et al., 2019). Indeed high winter nutrient fluxes are accompanied by high suspended solids, preventing algal growth (Guillaud et al., 2008).

Further, a positive N-ICEP in the Southern Biscay Bay coast did not lead to eutrophication problems at the coast, because the Gironde estuarine water fluxes are driven to the middle of the bay and those of the Adour spread throughout the Basque Country, especially at higher discharges (Ménesguen et al., 2018a). However, for the Charente estuary, which flows into the close Marennes-Oléron Bight, well known for oyster production, chronic summer mortality of "juveniles" was reported in the late 1990s to the early 2000s (Soletchnik et al., 2007). Garnier et al. (2021) demonstrated that the manifestations of

https://doi.org/10.5194/bg-2021-164
Preprint. Discussion started: 28 June 2021

560 eutrophication at the coast of riverine deliveries (and the associated ICEP) not only depends on the nutrient fluxes and their stoichiometry, but also on the morphology of the receiving media.

5. Conclusions

The 1-D biogeochemical model (C-GEM) was applied to seven estuaries with different sizes and morphologies along the French Atlantic coast (the Somme, Seine, Vilaine, Loire, Charente, Gironde, and Adour). Transient simulations were 565 implemented on water quality variables (PO_4, NH_4, NO_3, DSi, TOC, DO, and Chl-a) for 3 years (2014–2016). The model was calibrated and validated by comparing it with in situ sampling data along the estuaries. The results showed that this model presented accurate descriptions of the hydrodynamics, transport, and biogeochemistry in tidal estuaries, using simplified representations of the estuarine geometry and the same set of biogeochemical parameters for all estuaries.

C-GEM also quantifies the nutrient fluxes imported to and exported by the estuaries, reflecting human activities in the 570 upstream watersheds (population, agriculture). The retention rates for TP, TN, DSi, and TOC for the estuaries studied showed that large estuaries generally had a higher retention rate due to their longer residence times. Longer residence time provides enough time for biogeochemical reactions, thus reducing the fluxes of nutrients delivered to the sea. However, eutrophication does not only depend on nutrient fluxes, but also on their balance or imbalance. Therefore, the indicator for coastal eutrophication (ICEP) was evaluated for these seven estuaries, and indicated that for these estuaries, although no risk 575 appears regarding P, there might be a risk of coastal eutrophication due to the excess TN over DSi, and thus the development of potentially harmful nonsiliceous algae.

The present study thus provides a new understanding of the complex biogeochemical behavior of a range of estuaries. C-GEM can be combined with river models to simulate future scenarios with different degrees of anthropogenic impacts on the upstream basins, and, in turn, to assess how the estuaries would respond to potential or forthcoming disturbances.

580

Data availability. The measured data used in this study can be accessed through the links in section 2.2. C-GEM source code is available upon reasonable request to the corresponding authors.

Supplement.

Author contribution. XW constructed the data set, performed the simulations, analyzed the data, prepared the figures and 585 wrote the paper. JG GGL conceptualized and supervised this study, provided data, and completed, modified and revised the paper. VT, PP and RLG provided data for the dataset used for this study and revised the paper. GB and MA revised this paper.

Competing interests. The authors declare that they have no conflict of interest.

Acknowledgments.

590 ***Financial support.*** This study (Prest'Eaux project) was supported by the Office Français de la Biodiversité (OFB), greatly acknowledged for the project follow-up. Xi Wei's post-doc was funded by this project. Josette Garnier, Research Director at

https://doi.org/10.5194/bg-2021-164
Preprint. Discussion started: 28 June 2021

the CNRS, was the PI of Prest'Eaux. Goulven G. Laruelle is a research associate of the FRS-FNRS at the Université Libre de Bruxelles and contributed to the development of G-GEM.

References:

595 Arndt, S., Regnier, P. and Vanderborght, J. P.: Seasonally-resolved nutrient export fluxes and filtering capacities in a macrotidal estuary, J. Mar. Syst., 78(1), 42–58, doi:10.1016/j.jmarsys.2009.02.008, 2009.

Arndt, S., Lacroix, G., Gypens, N., Regnier, P. and Lancelot, C.: Nutrient dynamics and phytoplankton development along an estuary–coastal zone continuum: A model study, J. Mar. Syst., 84(3–4), 49–66, doi:10.1016/j.jmarsys.2010.08.005, 2011.

Baker, A.: Land Use and Water Quality, in Encyclopedia of Hydrological Sciences, vol. 12, p. 2412, John Wiley & Sons,
600 Ltd, Chichester, UK., 2005.

Barbier, E. B., Hacker, S. D., Kennedy, C., Koch, E. W., Stier, A. C. and Silliman, B. R.: The value of estuarine and coastal ecosystem services, Ecol. Monogr., 81(2), 169–193, doi:10.1890/10-1510.1, 2011.

Billen, G. and Garnier, J.: The Phison River plume: Coastal eutrophication in response to changes in land use and water management in the watershed, Aquat. Microb. Ecol., 13(1), 3–17, doi:10.3354/ame013003, 1997.

605 Billen, G. and Garnier, J.: River basin nutrient delivery to the coastal sea: Assessing its potential to sustain new production of non-siliceous algae, Mar. Chem., 106(1-2 SPEC. ISS.), 148–160, doi:10.1016/j.marchem.2006.12.017, 2007.

Brzezinski, M. A.: THE Si:C:N RATIO OF MARINE DIATOMS: INTERSPECIFIC VARIABILITY AND THE EFFECT OF SOME ENVIRONMENTAL VARIABLES, J. Phycol., 21(3), 347–357, doi:10.1111/j.0022-3646.1985.00347.x, 1985.

Coynel, A., Seyler, P., Etcheber, H. and Meybeck, M.: Spatial and seasonal dynamics of total suspended sediment and
610 organic carbon species in the Congo River, , 19(2), 1–17, doi:10.1029/2004GB002335, 2005.

Coynel, A., Gorse, L., Curti, C., Schafer, J., Grosbois, C., Morelli, G., Ducassou, E., Blanc, G., Maillet, G. M. and Mojtahid, M.: Spatial distribution of trace elements in the surface sediments of a major European estuary (Loire Estuary, France): Source identification and evaluation of anthropogenic contribution, J. Sea Res., 118, 77–91, doi:10.1016/j.seares.2016.08.005, 2016.

615 Crossland, C. J., Kremer, H. H., Lindeboom, H. J., Marshal Crosslandl, J. I. and Le Tissier, M. D. A.: Coastal Fluxes in the Anthropocene, edited by C. J. Crossland, H. H. Kremer, H. J. Lindeboom, J. I. Marshall Crossland, and M. D. A. Le Tissier, Springer Berlin Heidelberg, Berlin, Heidelberg., 2005.

Cugier, P., Billen, G., Guillaud, J. F., Garnier, J. and Ménesguen, A.: Modelling the eutrophication of the Seine Bight (France) under historical, present and future riverine nutrient loading, J. Hydrol., 304(1–4), 381–396,
620 doi:10.1016/j.jhydrol.2004.07.049, 2005a.

Cugier, P., Ménesguen, A. and Guillaud, J. F.: Three-dimensional (3D) ecological modelling of the Bay of Seine (English Channel, France), J. Sea Res., 54(1), 104–124, doi:10.1016/j.seares.2005.02.009, 2005b.

Defontaine, S., Sous, D., Morichon, D., Verney, R. and Monperrus, M.: Hydrodynamics and SPM transport in an engineered tidal estuary: The Adour river (France), Estuar. Coast. Shelf Sci., 231(January), 106445, doi:10.1016/j.ecss.2019.106445,
625 2019.

Dürr, H. H., Laruelle, G. G., van Kempen, C. M., Slomp, C. P., Meybeck, M. and Middelkoop, H.: Worldwide Typology of Nearshore Coastal Systems: Defining the Estuarine Filter of River Inputs to the Oceans, Estuaries and Coasts, 34(3), 441–

458, doi:10.1007/s12237-011-9381-y, 2011.

Escolano, J. J., Pedreño, J. N., Lucas, I. G., Almendro Candel, M. B. and Zorpas, A. A.: Decreased Organic Carbon Associated With Land Management in Mediterranean Environments. Report From the Commission to the European Parliament, the Council., Elsevier Inc., 2018.

Etcheber, H., Taillez, A., Abril, G., Garnier, J., Servais, P., Moatar, F. and Commarieu, M. V.: Particulate organic carbon in the estuarine turbidity maxima of the Gironde, Loire and Seine estuaries: Origin and lability, Hydrobiologia, 588(1), 245–259, doi:10.1007/s10750-007-0667-9, 2007.

Gallego-Sala, A., Goddéris, Y., Goossens, N., Hartmann, J., Heinze, C., Ilyina, T., Joos, F., Larowe, D. E., Leifeld, J., Meysman, F. J. R., Munhoven, G., Raymond, P. A., Spahni, R., Suntharalingam, P. and

Garnier, J., Billen, G. and Cébron, A.: Modelling nitrogen transformations in the lower Seine river and estuary (France): impact of wastewater release on oxygenation and N2O emission, Hydrobiologia, 588(1), 291–302, doi:10.1007/s10750-007-0670-1, 2007.

Garnier, J., Billen, G., Even, S., Etcheber, H. and Servais, P.: Organic matter dynamics and budgets in the turbidity maximum zone of the Seine Estuary (France), Estuar. Coast. Shelf Sci., 77(1), 150–162, doi:10.1016/j.ecss.2007.09.019, 2008.

Garnier, J., Beusen, A., Thieu, V., Billen, G. and Bouwman, L.: N:P:Si nutrient export ratios and ecological consequences in coastal seas evaluated by the ICEP approach, Global Biogeochem. Cycles, 24(4), n/a-n/a, doi:10.1029/2009GB003583, 2010a.

Garnier, J., Billen, G., Némery, J. and Sebilo, M.: Transformations of nutrients (N, P, Si) in the turbidity maximum zone of the Seine estuary and export to the sea, Estuar. Coast. Shelf Sci., 90(3), 129–141, doi:10.1016/j.ecss.2010.07.012, 2010b.

Garnier, J., Riou, P., Le Gendre, R., Ramarson, A., Billen, G., Cugier, P., Schapira, M., Théry, S., Thieu, V. and Ménesguen, A.: Managing the Agri-Food System of Watersheds to Combat Coastal Eutrophication: A Land-to-Sea Modelling Approach to the French Coastal English Channel, Geosciences, 9(10), 441, doi:10.3390/geosciences9100441, 2019.

Garnier, J., Billen, G., Lassaletta, L., Vigiak, O., Nikolaidis, N. P. and Grizzetti, B.: Hydromorphology of coastal zone and structure of watershed agro-food system are main determinants of coastal eutrophication, Environ. Res. Lett., 16(2), 023005, doi:10.1088/1748-9326/abc777, 2021.

Glibert, P. M.: Harmful algae at the complex nexus of eutrophication and climate change, Harmful Algae, 91(March 2019), 101583, doi:10.1016/j.hal.2019.03.001, 2020.

Gohin, F., Van der Zande, D., Tilstone, G., Eleveld, M. A., Lefebvre, A., Andrieux-Loyer, F., Blauw, A. N., Bryère, P., Devreker, D., Garnesson, P., Hernández Fariñas, T., Lamaury, Y., Lampert, L., Lavigne, H., Menet-Nedelec, F., Pardo, S. and Saulquin, B.: Twenty years of satellite and in situ observations of surface chlorophyll-a from the northern Bay of Biscay to the eastern English Channel. Is the water quality improving?, Remote Sens. Environ., 233(September), 111343, doi:10.1016/j.rse.2019.111343, 2019.

Goubert, E., Menier, D., Traini, C., Mathew, M. J. and Gall, R. Le: Recent Morphobathymetrical Changes of the Vilaine Estuary (South Brittany , France): Discrimination of Natural and Anthropogenic Forcings and Assessment for Future Trends, Elsevier Inc., 2019.

Guillaud, J.-F., Aminot, A., Delmas, D., Gohin, F., Lunven, M., Labry, C. and Herbland, A.: Seasonal variation of riverine nutrient inputs in the northern Bay of Biscay (France), and patterns of marine phytoplankton response, J. Mar. Syst., 72(1–4),

309–319, doi:10.1016/j.jmarsys.2007.03.010, 2008.

Hofmann, A. F., Soetaert, K. and Middelburg, J. J.: Present nitrogen and carbon dynamics in the Scheldt estuary using a novel 1-D model, Biogeosciences, 5(4), 981–1006, doi:10.5194/bg-5-981-2008, 2008.

Howarth, R., Chan, F., Conley, D. J., Garnier, J., Doney, S. C., Marino, R. and Billen, G.: Coupled biogeochemical cycles: Eutrophication and hypoxia in temperate estuaries and coastal marine ecosystems, Front. Ecol. Environ., 9(1), 18–26, doi:10.1890/100008, 2011.

Howarth, R. W., Fruci, J. R. and Sherman, D.: Inputs of Sediment and Carbon to an Estuarine Ecosystem: Influence of Land Use, Ecol. Appl., 1(1), 27–39, doi:10.2307/1941845, 1991.

Hu, J. and Li, S.: Modeling the mass fluxes and transformations of nutrients in the Pearl River Delta, China, J. Mar. Syst., 78(1), 146–167, doi:10.1016/j.jmarsys.2009.05.001, 2009.

Husson, B., Hernández-Fariñas, T., Le Gendre, R., Schapira, M. and Chapelle, A.: Two decades of Pseudo-nitzschia spp. blooms and king scallop (Pecten maximus) contamination by domoic acid along the French Atlantic and English Channel coasts: Seasonal dynamics, spatial heterogeneity and interannual variability, Harmful Algae, 51, 26–39, doi:10.1016/j.hal.2015.10.017, 2016.

INSEE: Populations légales 2014. [online] Available from: https://www.insee.fr/fr/statistiques/2525755?sommaire=2525768#consulter-sommaire, 2014.

Jakobsen, H. H., J. Carstensen, P. J. Harrison, and Zingone, A. : Estimating time series phytoplankton biomass: Species identifications and comparing volume to carbon scaling ratios. Estuar. Coast. Shelf Sci. 162: 143–150. doi:10.1016/j.ecss.2015.05.006, 2015

Jay, D. A., Uncles, R. J., Largier, J., Geyer, W. R., Vallino, J. and Boynton, W. R.: A Review of Recent Developments in Estuarine Scalar Flux Estimation, Estuaries, 20(2), 262, doi:10.2307/1352342, 1997.

Kaiser, D., Unger, D., Qiu, G., Zhou, H. and Gan, H.: Natural and human influences on nutrient transport through a small subtropical Chinese estuary, Sci. Total Environ., 450–451, 92–107, doi:10.1016/j.scitotenv.2013.01.096, 2013.

Kobori, H., Taga, N.: Phosphatase activity and its role in the mineralization of organic phosphorus in coastal sea water. J. exp. mar. Bid. Ecol., 36, pp. 23-39, 1979.

Labry, C.; Delmas, D., Youenou, A., Quere, J., Leynaert A., Fraisse, S., Raimonet, M., Ragueneau O.: High alkaline phosphatase activity in phosphate replete waters: The case of two macrotidal estuaries. Limnol. Oceanogr. 61, 1513–1529, 2016.

Lajaunie-Salla, K., Wild-Allen, K., Sottolichio, A., Thouvenin, B., Litrico, X. and Abril, G.: Impact of urban effluents on summer hypoxia in the highly turbid Gironde Estuary, applying a 3D model coupling hydrodynamics, sediment transport and biogeochemical processes, J. Mar. Syst., 174, 89–105, doi:10.1016/j.jmarsys.2017.05.009, 2017.

Lamy, D., Artigas, L. F., Jauzein, C., Lizon, F. and Cornille, V.: Coastal bacterial viability and production in the eastern English Channel: A case study during a Phaeocystis globosa bloom, J. Sea Res., 56(3), 227–238, doi:10.1016/j.seares.2006.04.003, 2006.

Laruelle, G. G., Goossens, N., Arndt, S., Cai, W. J. and Regnier, P.: Air-water CO2 evasion from US East Coast estuaries, Biogeosciences, 14(9), 2441–2468, doi:10.5194/bg-14-2441-2017, 2017.

Laruelle, G. G., Marescaux, A., Gendre, R. Le, Garnier, J., Rabouille, C., Thieu, V. and Lehrter, J. C.: Carbon Dynamics Along the Seine River Network : Insight From a Coupled Estuarine / River Modeling Approach, , 6(April), 1–16,

doi:10.3389/fmars.2019.00216, 2019.

Lazure, P. and Dumas, F.: An external–internal mode coupling for a 3D hydrodynamical model for applications at regional scale (MARS), Adv. Water Resour., 31(2), 233–250, doi:10.1016/j.advwatres.2007.06.010, 2008.

Lefebvre, A., Guiselin, N., Barbet, F. and Artigas, F. L.: Long-term hydrological and phytoplankton monitoring (1992–2007) of three potentially eutrophic systems in the eastern English Channel and the Southern Bight of the North Sea, ICES J. Mar. Sci., 68(10), 2029–2043, doi:10.1093/icesjms/fsr149, 2011.

Liquete, C., Piroddi, C., Drakou, E. G., Gurney, L., Katsanevakis, S., Charef, A. and Egoh, B.: Current Status and Future Prospects for the Assessment of Marine and Coastal Ecosystem Services: A Systematic Review, edited by S. J. Bograd, PLoS One, 8(7), e67737, doi:10.1371/journal.pone.0067737, 2013.

Luu, T. N. M., Garnier, J., Billen, G., Le, T. P. Q., Nemery, J., Orange, D. and Le, L. A.: N, P, Si budgets for the Red River Delta (northern Vietnam): How the delta affects river nutrient delivery to the sea, Biogeochemistry, 107(1–3), 241–259, doi:10.1007/s10533-010-9549-8, 2012.

McLean, M. J., Mouillot, D., Goascoz, N., Schlaich, I. and Auber, A.: Functional reorganization of marine fish nurseries under climate warming, Glob. Chang. Biol., 25(2), 660–674, doi:10.1111/gcb.14501, 2019.

Ménesguen, A., Dussauze, M. and Dumas, F.: Designing optimal scenarios of nutrient loading reduction in a WFD/MSFD perspective by using passive tracers in a biogeochemical-3D model of the English Channel/Bay of Biscay area, Ocean Coast. Manag., 163(May), 37–53, doi:10.1016/j.ocecoaman.2018.06.005, 2018a.

Ménesguen, A., Desmit, X., Dulière, V., Lacroix, G., Thouvenin, B., Thieu, V. and Dussauze, M.: How to avoid eutrophication in coastal seas? A new approach to derive river-specific combined nitrate and phosphate maximum concentrations, Sci. Total Environ., 628–629, 400–414, doi:10.1016/j.scitotenv.2018.02.025, 2018b.

Ménesguen, A., Dussauze, M., Dumas, F., Thouvenin, B., Garnier, V., Lecornu, F. and Répécaud, M.: Ecological model of the Bay of Biscay and English Channel shelf for environmental status assessment part 1: Nutrients, phytoplankton and oxygen, Ocean Model., 133(November 2018), 56–78, doi:10.1016/j.ocemod.2018.11.002, 2019.

Michel, P., Boutier, B. and Chiffoleau, J. F.: Net fluxes of dissolved arsenic, cadmium, copper, zinc, nitrogen and phosphorus from the Gironde Estuary (France): Seasonal variations and trends, Estuar. Coast. Shelf Sci., 51(4), 451–462, doi:10.1006/ecss.2000.0691, 2000.

Modéran, J., David, V., Bouvais, P., Richard, P. and Fichet, D.: Organic matter exploitation in a highly turbid environment: Planktonic food web in the Charente estuary, France, Estuar. Coast. Shelf Sci., 98, 126–137, doi:10.1016/j.ecss.2011.12.018, 2012.

Moriasi, D. N., Arnold, J. G., Van Liew, M. W., Bingner, R. L., Harmel, R. D. and Veith, T. L.: Model Evaluation Guidelines for Systematic Quantification of Accuracy in Watershed Simulations, Trans. ASABE, 50(3), 885–900, doi:10.13031/2013.23153, 2007.

Nguyen, A. T., Némery, J., Gratiot, N., Garnier, J., Dao, T. S., Thieu, V. and Laruelle, G. G.: Biogeochemical functioning of an urbanized tropical estuary: Implementing the generic C-GEM (reactive transport) model, Sci. Total Environ., 784, 147261, doi:10.1016/j.scitotenv.2021.147261, 2021.

Nguyen, T. T. N., Némery, J., Gratiot, N., Garnier, J., Strady, E., Tran, V. Q., Nguyen, A. T., Nguyen, T. N. T., Golliet, C. and Aimé, J.: Phosphorus adsorption/desorption processes in the tropical Saigon River estuary (Southern Vietnam) impacted by a megacity, Estuar. Coast. Shelf Sci., 227(July), 106321, doi:10.1016/j.ecss.2019.106321, 2019.

Nixon, S. W., Ammerman, J. W., Atkinson, L. P., Berounsky, V. M., Billen, G., Boicourt, W. C., Boynton, W. R., Church, T.

M., Ditoro, D. M., Elmgren, R., Garber, J. H., Giblin, A. E., Jahnke, R. A., Owens, N. J. P., Pilson, M. E. Q. and Seitzinger, S. P.: The fate of nitrogen and phosphorus at the land-sea margin of the North Atlantic Ocean, Biogeochemistry, 35(1), 141–180, doi:10.1007/BF02179826, 1996.

Normandin, C., Lubac, B., Sottolichio, A., Frappart, F., Ygorra, B. and Marieu, V.: Analysis of Suspended Sediment Variability in a Large Highly Turbid Estuary Using a 5-Year-Long Remotely Sensed Data Archive at High Resolution, J. Geophys. Res. Ocean., 124(11), 7661–7682, doi:10.1029/2019JC015417, 2019.

Perez, B. C., Day, J. W., Justic, D., Lane, R. R. and Twilley, R. R.: Nutrient stoichiometry, freshwater residence time, and nutrient retention in a river-dominated estuary in the Mississippi delta, Hydrobiologia, 658(1), 41–54, doi:10.1007/s10750-010-0472-8, 2011.

Pozdnyakov, D. V, Pettersson, L. H. and Korosov, A. A.: Exploring the Marine Ecology from Space, Springer International Publishing, Cham., 2017.

Pritchard, D. W.: What is an estuary: physical viewpoint, In Estuaries. AAAS, Washington DC., 1967.

Ragueneau, O., Lancelot, C., Egorov, V., Vervlimmeren, J., Cociasu, A., Déliat, G., Krastev, A., Daoud, N., Rousseau, V., Popovitchev, V., Brion, N., Popa, L., Cauwet, G.: Biogeochemical transformations of inorganic nutrients in the mixing zone between the Danube River and the North-western Black Sea. Estuarine, Coastal and Shelf Science 54, 321-336, 2002.

Ratmaya, W., Soudant, D., Salmon-Monviola, J., Plus, M., Cochennec-Laureau, N., Goubert, E., Andrieux-Loyer, F., Barillé, L. and Souchu, P.: Reduced phosphorus loads from the Loire and Vilaine rivers were accompanied by increasing eutrophication in the Vilaine Bay (south Brittany, France), Biogeosciences, 16(6), 1361–1380, doi:10.5194/bg-16-1361-2019, 2019.

Redfield, A. C., Ketchum, B. H. and Richards, F. A.: The Influence of Organisms on the Composition of the Sea Water, in Hill MN (ed) The Sea, edited by M. N. Hill, pp. 12–17, John Wiley & Sons, Inc., New York., 1963.

Regnier, P., Mouchet, A., Wollast, R. and Ronday, F.: A discussion of methods for estimating residual fluxes in strong tidal estuaries, Cont. Shelf Res., 18(13), 1543–1571, doi:10.1016/S0278-4343(98)00071-5, 1998.

Regnier, P., Friedlingstein, P., Ciais, P., Mackenzie, F. T., Gruber, N., Janssens, I. A., Laruelle, G. G., Lauerwald, R., Luyssaert, S., Andersson, A. J., Arndt, S., Arnosti, C., Borges, A. V., Dale, A. W.,

REPHY: French Observation and Monitoring program for Phytoplankton and Hydrology in coastal waters. Metropolitan data., SEANOE, doi:https://doi.org/10.17882/47248, 2021.

Romero, E., Garnier, J., Lassaletta, L., Billen, G., Le Gendre, R., Riou, P. and Cugier, P.: Large-scale patterns of river inputs in southwestern Europe: Seasonal and interannual variations and potential eutrophication effects at the coastal zone, Biogeochemistry, 113(1–3), 481–505, doi:10.1007/s10533-012-9778-0, 2013.

Romero, E., Le Gendre, R., Garnier, J., Billen, G., Fisson, C., Silvestre, M. and Riou, P.: Long-term water quality in the lower Seine: Lessons learned over 4 decades of monitoring, Environ. Sci. Policy, 58, 141–154, doi:10.1016/j.envsci.2016.01.016, 2016.

Romero, E., Garnier, J., Billen, G., Ramarson, A., Riou, P. and Le Gendre, R.: Modeling the biogeochemical functioning of the Seine estuary and its coastal zone: Export, retention, and transformations, Limnol. Oceanogr., 64(3), 895–912, doi:10.1002/lno.11082, 2019.

Roubeix, V., Rousseau, V., and Lancelot, C.: Diatom succession and silicon removal from freshwater in estuarine mixing zones: From experiment to modelling. Estuarine, Coastal and Shelf Science 78 14-26, 2008.

Savenije, H. H. G.: Salinity and tides in alluvial estuaries. [online] Available from: http://hubertsavenije.files.wordpress.com/2014/01/salinityandtides2_21.pdf, 2012.

Savoye, N., David, V., Morisseau, F., Etcheber, H., Abril, G., Billy, I., Charlier, K., Oggian, G., Derriennic, H. and Sautour, B.: Origin and composition of particulate organic matter in a macrotidal turbid estuary: The Gironde Estuary, France, Estuar. Coast. Shelf Sci., 108, 16–28, doi:10.1016/j.ecss.2011.12.005, 2012.

Seitzinger, S., Harrison, J. A., Böhlke, J. K., Bouwman, A. F., Lowrance, R., Peterson, B., Tobias, C. and Van Drecht, G.: Denitrification across landscapes and waterscapes: a synthesis., Ecol. Appl., 16(6), 2064–90, doi:10.1890/1051-0761(2006)016[2064:dalawa]2.0.co;2, 2006.

Seitzinger, S. P.: Denitrification in freshwater and coastal marine ecosystems: Ecological and geochemical significance, Limnol. Oceanogr., 33(4,part2), 702–724, doi:10.4319/lo.1988.33.4part2.0702, 1988.

Soletchnik, P., Ropert, M., Mazurié, J., Gildas Fleury, P. and Le Coz, F.: Relationships between oyster mortality patterns and environmental data from monitoring databases along the coasts of France, Aquaculture, 271(1–4), 384–400, doi:10.1016/j.aquaculture.2007.02.049, 2007.

Thouvenin, B., Gonzalez, J. . and Boutier, B.: Modelling of pollutant behaviour in estuaries: Application to cadmium in the Loire estuary, Mar. Chem., 58(1–2), 147–161, doi:10.1016/S0304-4203(97)00031-5, 1997.

Thullner, M.: Anthropogenic perturbation of the carbon fluxes from land to ocean, Nat. Geosci., 6(8), 597–607, doi:10.1038/ngeo1830, 2013.

Toublanc, F., Brenon, I., Coulombier, T. and Le Moine, O.: Fortnightly tidal asymmetry inversions and perspectives on sediment dynamics in a macrotidal estuary (Charente, France), Cont. Shelf Res., 94, 42–54, doi:10.1016/j.csr.2014.12.009, 2015.

UE-SOeS CORINE Land Cover: L'occupation des sols en 2018. [online] Available from: https://www.insee.fr/fr/statistiques/2525755?sommaire=2525768#consulter-sommaire, 2018.

Vanderborght, J. P., Folmer, I. M., Aguilera, D. R., Uhrenholdt, T. and Regnier, P.: Reactive-transport modelling of C, N, and O2 in a river-estuarine-coastal zone system: Application to the Scheldt estuary, Mar. Chem., 106(1-2 SPEC. ISS.), 92–110, doi:10.1016/j.marchem.2006.06.006, 2007.

Verri, G., Mahmoudi Kurdistani, S., Coppini, G. and Valentini, A.: Recent Advances of a Box Model to Represent the Estuarine Dynamics: Time-Variable Estuary Length and Eddy Diffusivity, J. Adv. Model. Earth Syst., 13(4), 1–16, doi:10.1029/2020MS002276, 2021.

Vilas, F., Rubio, B., Rey, D. and Bernabeu, A. M.: Estuary, in Encyclopedia of Planetary Landforms, pp. 1–7, Springer New York, New York, NY., 2021.

Volta, C., Laruelle, G. G., Arndt, S. and Regnier, P.: C-GEM (v 1.0): a new, cost-efficient biogeochemical model for estuaries and its application to a funnel-shaped system, , (February 2016), doi:10.5194/gmd-7-1271-2014, 2014.

Volta, C., Laruelle, G. G., Arndt, S. and Regnier, P.: Linking biogeochemistry to hydro-geometrical variability in tidal estuaries: a generic modeling approach, Hydrol. Earth Syst. Sci., 20(3), 991–1030, doi:10.5194/hess-20-991-2016, 2016a.

Volta, C., Laruelle, G. G. and Regnier, P.: Regional carbon and CO2 budgets of North Sea tidal estuaries, Estuar. Coast. Shelf Sci., 176, 76–90, doi:10.1016/j.ecss.2016.04.007, 2016b.

Wild-Allen, K., Skerratt, J., Whitehead, J., Rizwi, F. and Parslow, J.: Mechanisms driving estuarine water quality: A 3D biogeochemical model forinformed management, Estuar. Coast. Shelf Sci., 135, 33–45, doi:10.1016/j.ecss.2013.04.009,

https://doi.org/10.5194/bg-2021-164
Preprint. Discussion started: 28 June 2021

2013.

825